RESPONSE OF REINFORCED CONCRETE BUILDING SUBJECTED TO NORTHRIDGE EARTHQUAKE

By
Sinique Betancourt Martínez
and
JoAnn Browning

A Report on Research Sponsored by

THE NATIONAL SCIENCE FOUNDATION
Research Grant No. 9904090

Structural Engineering and Engineering Materials
SM Report No. 67

UNIVERSITY OF KANSAS CENTER FOR RESEARCH, INC.
LAWRENCE, KANSAS
May 2002

RESPONSE OF REINFORCED CONCRETE BUILDING SUBJECTED TO NORTHRIDGE EARTHQUAKE

By

Sinique Betancourt Martínez

B.S., Universidad del Valle, Cali, Colombia, 1998

M.S., University of Kansas, Lawrence, Kansas, 2002

Submitted to the Department of Civil and Environmental Engineering and the Faculty of the Graduate School of the University of Kansas in partial fulfillment of the requirements for the degree of Master of Science.

Thesis Committee:

_____

Chairperson

_____

_____

Thesis defended April 19, 2002

RESPONSE OF REINFORCED CONCRETE BUILDING SUBJECTED TO NORTHRIDGE EARTHQUAKE

By
Sinique Betancourt Martínez
and
JoAnn Browning

A Report on Research Sponsored by

THE NATIONAL SCIENCE FOUNDATION
Research Grant No. 9904090

Structural Engineering and Engineering Materials
SM Report No. 67

UNIVERSITY OF KANSAS CENTER FOR RESEARCH, INC.
LAWRENCE, KANSAS
May 2002

ABSTRACT

The study of instrumented buildings helps to improve the understanding of how structures respond to earthquakes and to decrease losses due to damage in future earthquakes. Traditional methods for modeling reinforced concrete elements may be used to provide estimates of the building response, and these methods can then be evaluated based on the measured response. This study focuses on the modeling and response modification of a reinforced concrete building designed in 1964 and subjected to the 1994 Northridge earthquake. The significance of the study is the investigation of the response of a reinforced concrete building with poor detailing and subjected to moderate earthquake demands.

The structure is a reinforced concrete frame building located in Sherman Oaks, California with 13 stories and 2 sublevels. The building was instrumented with 15 sensors distributed on 5 floors. The maximum drift response of the structure was determined to be 0.7% of the total height of the structure with an associated maximum recorded ground acceleration of 0.23g. The study discusses the challenges of simulating the response of a structure having poorly detailed reinforced concrete columns that is subjected to moderate earthquake demands as well as how to apply a strength reduction factor to study the modification of the structural response.

ACKNOWLEDGEMENTS

First I would like to thank my advisor, Dr. JoAnn Browning, because she offered me the opportunity to participate in this research project and to study at the University of Kansas. I express my gratitude to Rebeccah N. Russell for her invaluable help in the development of this study.

I would like to express my gratitude to Professors Adolfo Matamoros and Mario Medina for serving in the evaluation committee.

This investigation was completed with the support of The National Science Foundation Graduate Fellowship and under grant # NSF 9904090, Dr. S.C. Liu, Program Director.

TABLE OF CONTENTS

LIST OF TABLES

LIST OF FIGURES

1. Introduction

1.1. Problem Statement

The detailing of elements of reinforced concrete frames for seismic regions requires that the anticipated maximum response (displacement) of the elements be estimated. For reinforced concrete (RC) frames, the yielded shape of the structure determined from non-linear analysis provides a useful tool for estimating the locations of maximum response in the building. A tool (a strength relationship) was previously developed to modify the locations of maximum response based on a study using hypothetical reinforced concrete frames and the response of a 7-story instrumented building (Kuntz, 2001). Using this tool, the yielded shape of the building is modified so that the maximum response in the elements occurs at higher locations where the axial stress is less harmful to the overall stability of the structure and the severity of damage to the elements is reduced. Although the strength relationship has been shown to be effective for the low-rise structure and the hypothetical frames, it is important to demonstrate the applicability of the method using moderate-rise frames. This thesis focuses on the modeling and response modification of a 13-story reinforced concrete frame.

1.2. Literature Review

There are several issues to consider when modeling RC structures: how to obtain the element properties, how to model the material properties, which hysteretic

model to use and what type of structural model is more suitable for the problem. During the past 40 years there have been several approaches to all of these issues, in the following sections each one will be addressed and discussed.

1.2.1. Element Properties

The FEMA 273 (1997) guidelines recommends a site visit to examine the physical condition of the structure and the surrounding structures or conditions that may have an influence on the structure. It specifies that for a non-linear dynamic procedure it is necessary to model the hysteresis behavior of each structural element using the actual properties of the member. The inelastic response should be restricted only to structural members. Only elements that have demonstrated that can support inelastic action may be included in the analysis. The modeling of concrete buildings may or may not include the foundation. If the foundation is not included in the model there are two options for the joint between column lines and foundation pile caps. One is assume a fix joint, in order to do that the foundation and bearing soil should be able to resist the induced moments. The other option is to model the joint as a pinned-end, this will require more analysis for the column elements. If the model includes the foundation a specific procedure should be follow.

1.2.2. Material Properties

A more recent approach is found in FEMA 273. It provides general guidelines on how to model different types of concrete structures and components. The guidelines specify minimum values for the material properties to use in the model depending upon the year in which the target structure was built, and recommends

using these values unless higher values are specified in the structural plans. These guidelines may be used in lieu of individual analysis of samples from the structure.

1.2.3. Hysteretic Models

There are many different approaches to the modeling of RC structures. The maiden attempts to model RC systems were made around the mid 60's. One of the first approaches was based on a bilinear hysteretic model. It was found that the behavior of a reinforced concrete member was complex and a bilinear elastic hysteresis model did not accurate simulate the behavior. Clough and Johnston developed a degrading stiffness model in 1966, that considered the stiffness reduction at load-reversals. This model assumes that both the initial stiffness and the unloading stiffness have the same value despite of the presence of structural damage. The stiffness degradation is simulated as deformation in the Clough model, the response point have to reach a limit response in the direction of the loading. The way the stiffness degradation was represented was found to be a weakness of the Clough model. If unloading occurs before the maximum response point the Clough model assumed that the point should move directly to the maximum response point, this was not suitable, it was more likely that the point move toward the unloading point first and after move toward the maximum response point. In 1970, Takeda, Sozen and Nielsen., introduced the degrading stiffness scheme to represent the behavior observed in experimental results. This model introduced stiffness changes at cracking, yielding and unloading stiffness degradation with deformation. This became a widely used model for non-linear analysis of RC structures. This model may be used as a

bilinear model when the cracking stiffness is assumed to be zero, when that occurs the Takeda model is very similar to Clough model, the only difference is some additional rules that the Takeda model requires to use. A trilinear hysteresis method was implemented by Otani and Sozen (1972), in which they highlighted the importance of monitoring the inflexion point.

1.2.4. Structural and Soil Models

The two most common models used are stick models and finite element models (FEM). Both models will have a general description in the following paragraphs. Both of these modeling approaches are used for structural models and soil-structure interaction models.

1.2.4.1. Stick Models

In general the stick models represent each structural element as a massless stick with springs at the ends or some kind of joint among elements and the mass may be lumped at either the element midspan or for each degree of freedom (Saiidi, 1979, Lopez,1988). Depending on which routine is being used the springs may represent the non-linear and inelastic element properties, the elasto-plastic behavior of the elements or both. To represent the soil properties the stick models use a spring that represent the rocking stiffness of the soil (Chowdhury, 1984). A more in depth explanation on how the stick model used for this study works is discussed in sections 3.2 and 3.3.

1.2.4.2. Finite Element Models

This domain method represents the continous elastic structure with a finite number of degrees of freedom. The structure is discretized in small well defined

elements that have different material and geometry properties depending on which part of the continuum it is representing. Each element has nodes, the nodes are the places where the elements have contact with the other elements or boundaries. Is at the nodes where the loads and boundary conditions and elastic properties are assigned and applied. In the nodes is where the degree of freedom are located and the can be translational or rotational, each node can have at the most 6 degrees of freedom (3 rotational and 3 translational). Each element is defined by a local matrix, after each element has been defined all the elements are assembled in a global matrix using the common nodes to create the overall matrix. After this step the loads and boundary conditions are specified and after solving matrix calculations the deformations for the system are found. Using equations of elasticity and knowing the displacements is possible to find the stresses and strain values for specific points within the structure. There are different types of finite elements, among them are found: line elements, surface elements, solid elements, and special purpose elements. The use of each one of those depends upon the specific application in which they are going to be used. The representation of the soil properties using FEM is complex because the soil is an unbounded media and it can be modeled as a bounded media assuming specific nodal points or as an unbounded media where it is necessary to define an interaction horizon for the soil (Wolf, 1996).

1.3. Scope of Work

The thesis is developed in two parts. The first part deals with modeling a 13-story frame with 2 sublevels subjected to moderate levels of ground motion. The

second part focuses on applying the strength-based relationship to modify the response of the structure.

The general description of the target structure is discussed in Chapter 2. The focus of this chapter is the description of a reinforced concrete structure located in Sherman Oaks, California with 13 stories and 2 sublevels. The building was instrumented with 15 sensors distributed on 5 different floors. The maximum drift response of the structure was determined to be 0.7% of the total height of the structure with a maximum-recorded ground acceleration of 0.23g (Channel 13). The direction of maximum drift response (E-W) was chosen as the modeling direction, however the maximum ground acceleration value was recorded in the orthogonal direction (N-S) as 0.45 g.

The various models used in the analysis are discussed in Chapter 3. The target structure was modeled as two main frames (second sublevel to the roof) and an additional wall frame (2nd sublevel to the ground). Only two of the three main frames were modeled, recognizing that the exterior frames are nearly identical. The target structure presents several challenges for modeling the response recorded during the Northridge earthquake. The structure is a composed of an RC moment resisting frame for the superstructure and shear walls and frames for the substructure. During the modeling process, excessive roof drift noted in the recorded response was difficult to model and this was attributed to either the soil-structure interaction or the flexibility of the sublevels and foundation. These options were investigated as part of this study. Another issue was that some structural elements above the first floor

(girders and slabs) were built with lightweight concrete. This condition was taken into account for mass calculation and moment-curvature calculations.

Three models were evaluated in the study:

- An as-designed model based on the actual structural properties as described in the structural plans was modeled including the ground level and stories above. (Model A)
- An as-designed model based on the actual structural properties as described in the structural plans was modeled including all levels (Model B), and
- A model modified to reflect the flexibility of the walls and girders in the sublevels was modeled (Model C).

The models were compared to determine the best representation of the recorded response of building. The first model (Model A) include only the floors above ground level. This approach was taken because the displacement response below the ground was small (section 3.4.2.1). After analyzing the response of Model A, it was found that it did not adequately represent the behavior of the target structure, and it was necessary then to implement in the model the structural properties of the elements in the sublevels (Model B) (section 3.4.2.2). Even though Model B has all the actual structural properties of the building it did not represent the recorded response near the base very well. The discrepancy at the base was thought to be caused by either the stiffness of the sublevels of soil-structure interaction. It was necessary then to apply some modifications suggested by FEMA 273 for the modeling of concrete structures. A model (Model C) was developed and analyzed

with changes to the elements in the floors below ground. Model C represented the increased flexibility of the sublevels and the foundation (section 3.5.1).

The models including all levels were modified using the strength-based relationship as described in Chapter 4. The modifications were made to the strength of selected girders to determine the altered response of the structure for moderate and high earthquake demands. The strength of some the girders in models B and C was modified by a factor calculated with the following formula, which was developed by Kuntz (2001):

$$R = 1 + \frac{N_s \cdot N_b \cdot \sqrt{\rho \cdot h}}{7 \cdot (N_b + 1) \cdot \beta \cdot \alpha^2} \qquad (1.1)$$

The altered models were analyzed using dynamic routines and the responses were compared with the response of the original models.

Finally, the conclusions are presented in Chapter 5. After applying the relationship developed by Kuntz, it was found that the strength reduction factor did help to improve the response of Model B, which has a stiff foundation, but it did not improve the response of Model C. Three records were selected for the comparison of the structural response. The frequency content of the acceleration records used for the analyses apparently have an influence in the unmodified models response, which makes the reduction factor more or less effective on the model.

2. Description of the Target Structure

In the following pages the target structure will be describe in detail. The structural and material properties will be discussed. The instrumentation location will be shown as well as the registered damaged suffer by the structure. This will allow a better understanding of the structure and the study developed here.

2.1. Location

The target structure is a commercial building located in Sherman Oaks, CA. It was designed in 1964 and built in 1965 (Figure 2-1). The structure was located approximately 9 km (5.59 mi) southeast of the epicenter of the Northridge earthquake as shown in Figure 2-2 (MAPQUEST, 2001).

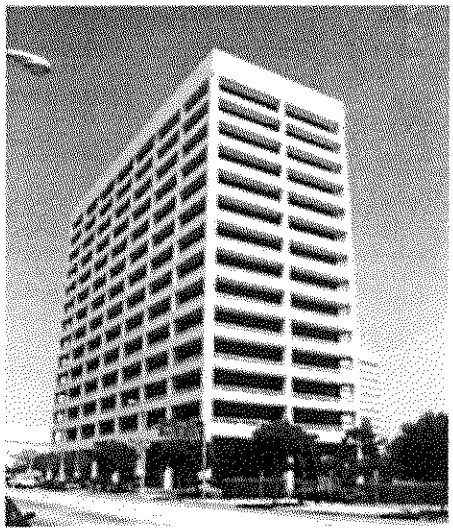

Figure 2-1. Target Structure (Naeim, 2000)

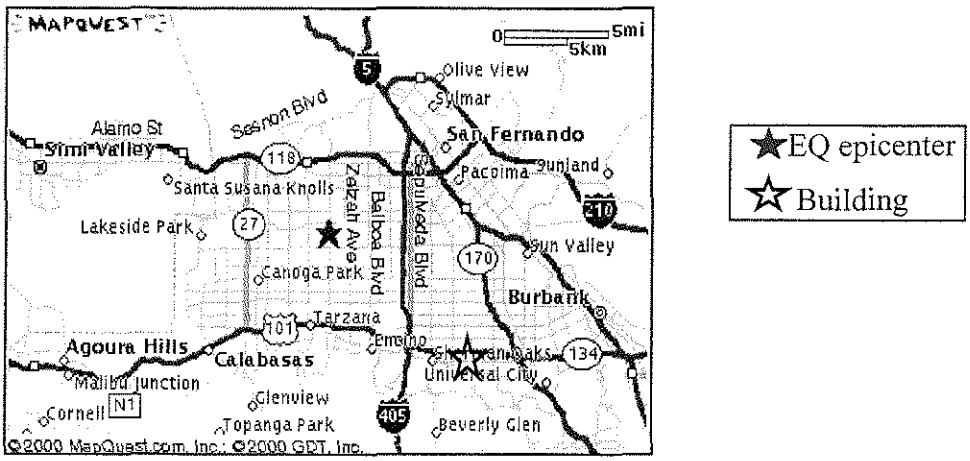

Figure 2-2. Earthquake and Target Structure Location (Mapquest 2001)

2.2. Structural Configuration

2.2.1. Building Layout

The building is a reinforced concrete frame structure with 13 stories above ground and 2 stories below. It is currently an office building. The first sublevel (below the first floor) is 3.5 m (11.5 ft) in height while the second sublevel is 2.74 m (9 ft). The first floor is 7 m (23 ft) in height and all the other floors above the ground

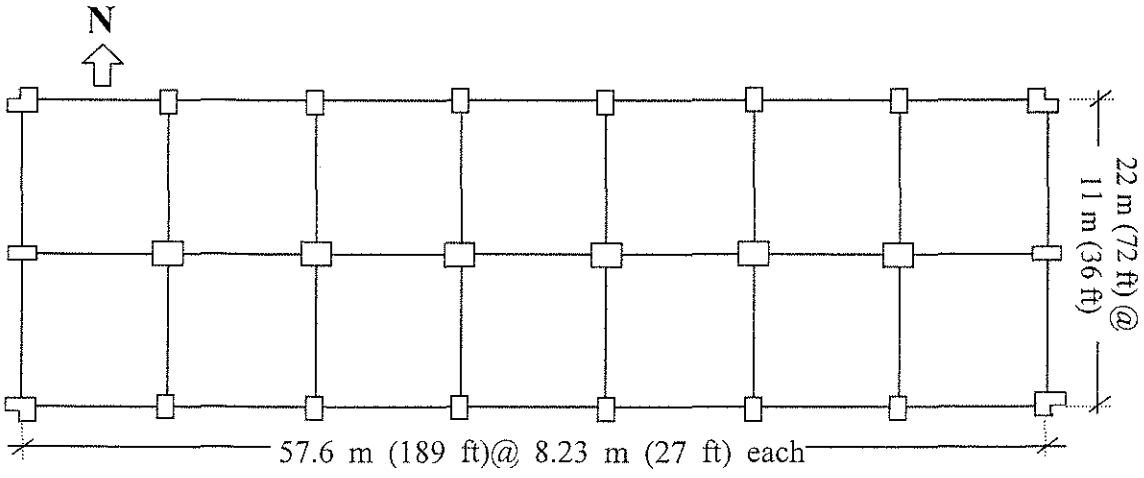

Figure 2-3. Typical Floor Plan (2nd floor to roof)

are 3.58 m (11.75 ft). As shown in Figure 2-3, in the N-S direction there are 8 frames and the E-W direction consists of 3 frames. The N-S frames have 2 bays spanning 11 m (36 ft) each, and the E-W frames have 7 bays spanning 8.23 m (27 ft) each. Consequently, each floor has an approximate area of 1267 m^2 (13608 ft^2). On the roof there is a penthouse for mechanical equipment, which contributes mass but not stiffness to the top level. There is a parking facility contiguous to the building. The elevation of the structure is shown in Figure 2-4.

The N-S direction consists of concrete moment resisting frames from the ground level through the roof level, and concrete shear walls in the sublevels. The structural configuration is similar for the E-W direction.

The load path consists of loads being transferred from the slab, to the intermediate beam, to the girders, to the columns and finally to the foundation. Each floor has a one-way concrete slab with a thickness of 114 mm (4.5 in).

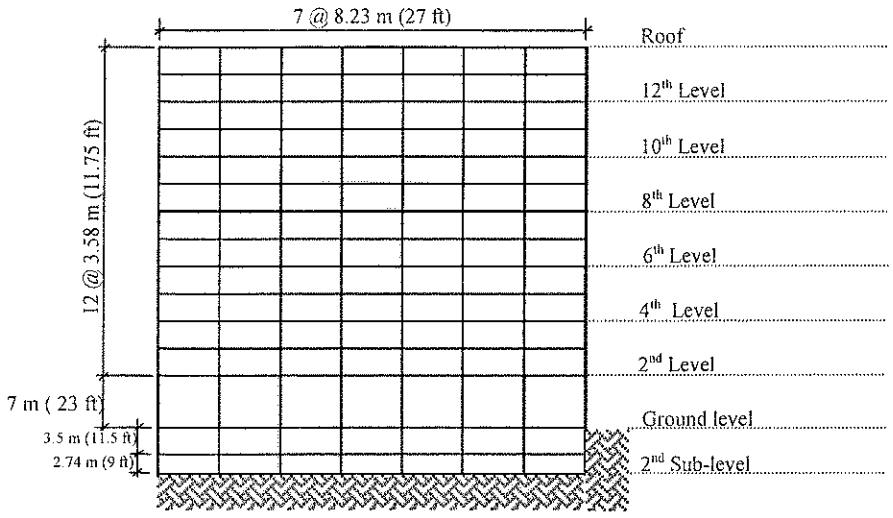

Figure 2-4. Structure Elevation Plan

2.2.2. Girders and Columns

The sizes of the girders vary throughout the height of the building and between frames, the actual cross sections are specified for the different frames below.

The exterior frames have 7 different girder sizes (width x height):

- **First floor underground** -The girder dimensions are 0.61 m x 0.61 m (24 in x 24 in) for all bays in south frame and the first 3 bays (from left to right) in north frame. The last 4 bays for the north frame have a girder section of 0.91 m x 0.61 m (36 in x 24 in) as shown by the dotted line in Figure 2-5.
- **Ground floor** - The girder dimensions are 0.76 m x 0.61 m (30 in x 24 in) for all bays in south frame. The north frame has two different girder sizes. The first one applies to the first 3 bays (from left to right) and its section is 0.53 m x 1.1 m (21 in x 42 in). The last 4 bays have girders with cross sectional area of 1.22 m x 0.69 m (48 in x 27 in), (Figure 2-5).
- **Second floor** - The girder dimensions are 0.46m. x 1.4 m (18 in x 55 in) for all bays in both of the frames.
- **Third floor and above** - The girder dimensions are 0.46 m. x 1 m. (18 in x 39 in) for all bays.

The interior frame has 6 different girder types, specified as follows:

- **First floor underground** - The girder dimensions are 0.61 m x 0.61 m (24 in x 24 in) for all bays.
- **Ground floor** - The girder dimensions are 0.76 m x 0.61 m (30 in x 24 in) for all bays.

- **Second floor** - The girder dimensions are 0.6 m x 0.9 m (24 in x 36 in.) for all bays.
- **Third floor to 13th floor** - The girders in the middle bay are 0.76 m x 0.47 m (30 in x 18.5 in), as shown by dark line in Figure 2-6, while all others are 0.6 m x 0.81 m (24 in x 32 in.).
- **Roof** - The girder dimensions are 0.6 m x 0.81 m. (24 in. x 32 in.) for all bays.

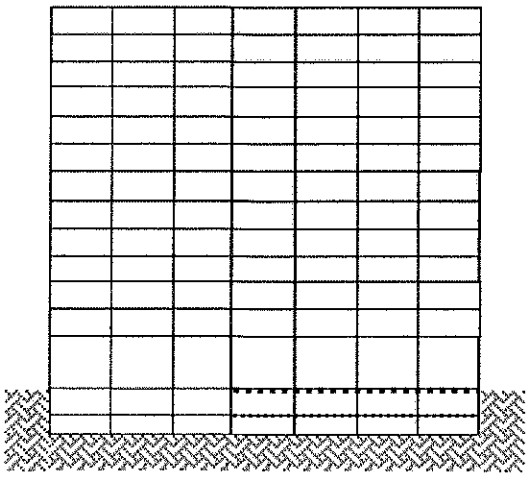

Figure 2-5. North Exterior Frame

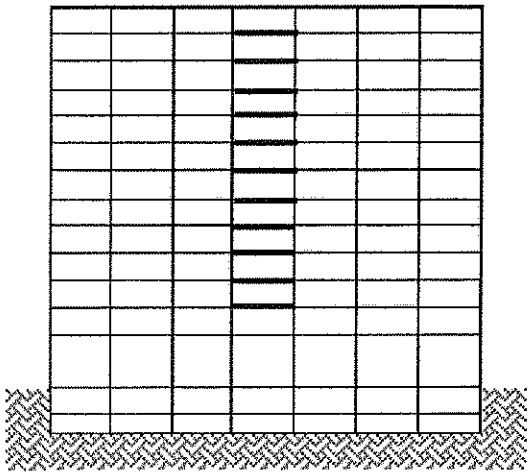

Figure 2-6. Interior Frame

Figure 2-7 shows the column distribution for the three frames for a typical floor plan. The exterior frames have two cross sections for the columns. The first cross section is 0.91 m. x 0.91 m. (36 in. x 36 in.) with a notch of 0.31 m. x 0.31 m. (12 in. x 12 in.) in the exterior corner. These columns are located in the corners of the structure. The second cross section has dimensions of 0.6 m x 0.9 m (24 in x 36 in.). The interior frame has exterior columns of 0.9 m x 0.6 m (36 in x 24 in) and interior columns of 0.91 m. x 0.91 m. (36 in. x 36 in.).

For sake of clarity, Figure 2-8 shows the column distribution for the three frames for the ground level and first sublevel. The exterior frames have only two

cross sections for columns while the interior frame has four cross sections for columns.

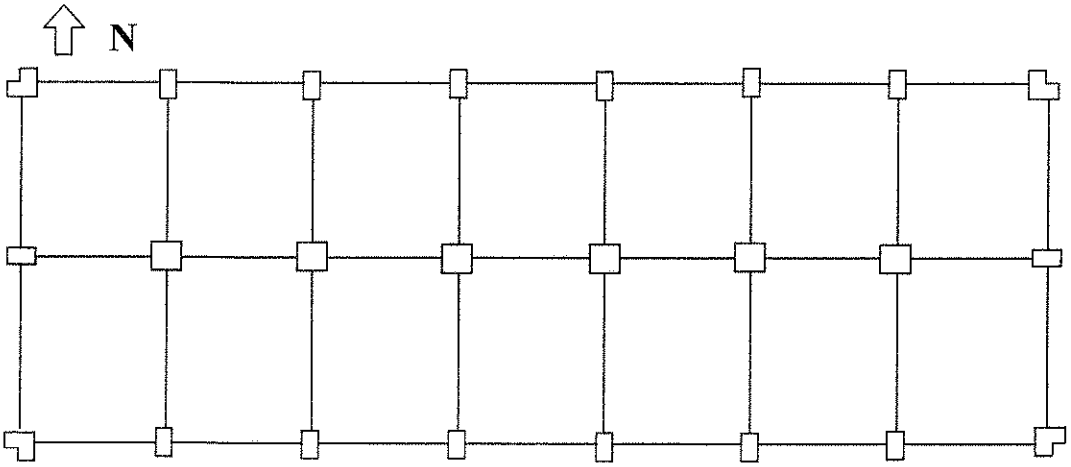

Figure 2-7. Columns In Typical Floor (2nd floor to roof)

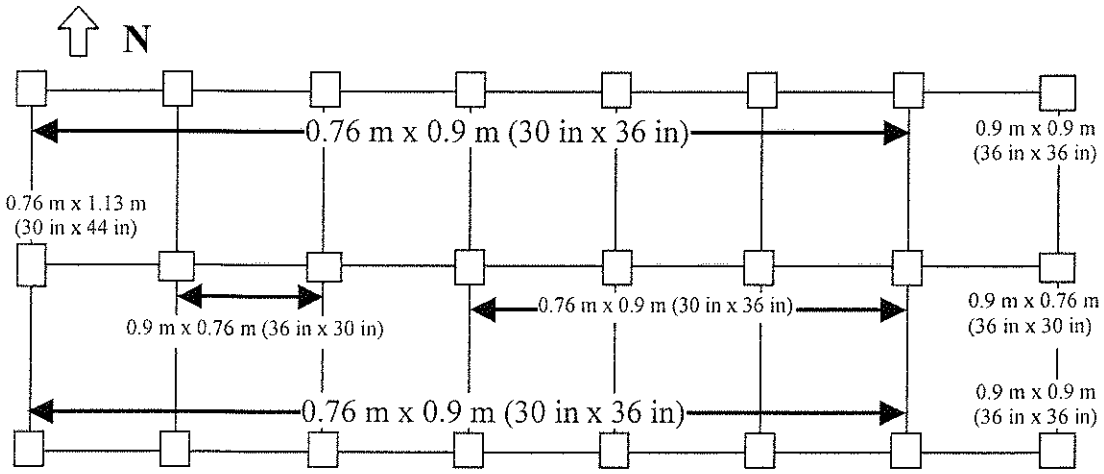

Figure 2-8. Column Distribution on Ground Level and 1st Sublevel

The non-structural elements consist of a curtain wall used as exterior cladding, partitions that are gypsum board on studs, and suspended acoustical tile acts as ceiling. Major fixed equipment is located in the basement and on the roof. The elevators are located between structural axis K and L (Figure 2-3).

2.3. Subsurface Conditions and Material Properties

The soil deposits supporting the structure are alluvium deposits from San Fernando Valley and are classified as clays, silt and sand (Naeim, 2000; Ventura et al, 1994). Shear walls surround the two sublevels offset from the frame by 2.44 m (8 ft), and connected by a 15.24 cm (6 in) slab. The foundation consists of concrete pile caps supporting each column line. Each pile cap groups between 12 and 23 piles. Most of the pile caps have an area of 27 m^2 (285 ft^2) and a height of 91 cm (3 ft). The length of the piles varies between 6 and 7.6 m (20 - 25 ft), depending upon the diameter of the pile. The diameter of the piles varies between 38 and 61 cm (15-24 inches).

The concrete used for columns and walls throughout the structure as well as floor elements below the second floor was regular weight. All other floor elements were constructed with lightweight concrete. The design strength for all columns was 34.5 MPa (5000 psi), and all girders had a design concrete strength of 25.8 MPa (3750 psi). Pile caps and piles had a concrete strength of 20.7 MPa (3000 psi).

2.4. Sensors

The structure was instrumented with 15 accelerometers distributed in 5 floors: three in the first level, three in the second level, three in the eighth level and three in the roof. Only one of the accelerometers recorded vertical accelerations (Ch.14).

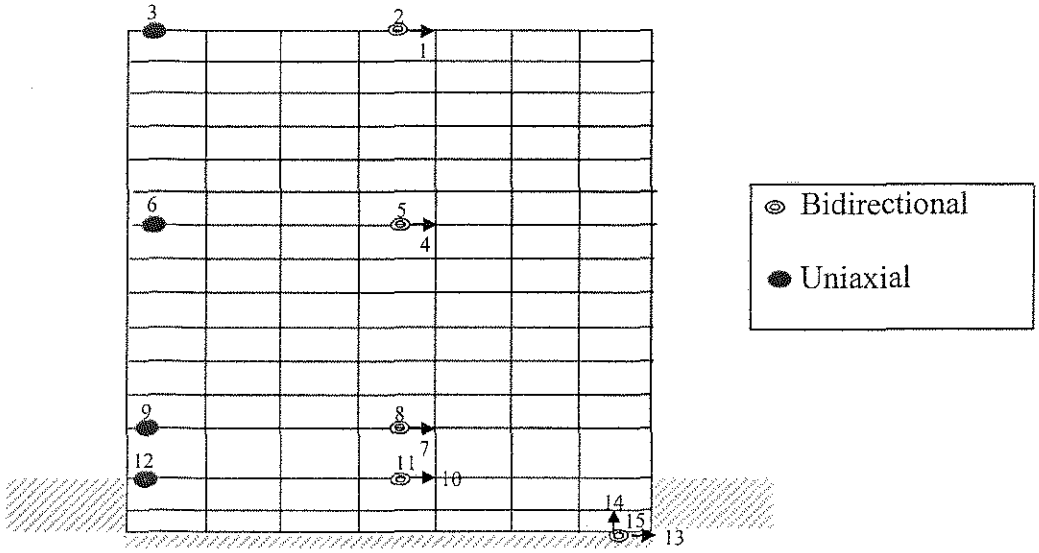

Figure 2-9. Sensor Locations (west – east)

Two types of accelerometers were used throughout the structure, manufactured by Kinemetrics Inc. The first model is called FBA-11. This is a uniaxial spring-mass device and is used on channels 3, 6, 9, and 12. The other model is FBA-23 and it is a multidirectional accelerometer. This model is used to collect acceleration values for different directions simultaneously. The data from the accelerometers is obtained through a data acquisition system. Figure 2-10 shows a picture of the model FBA-23.

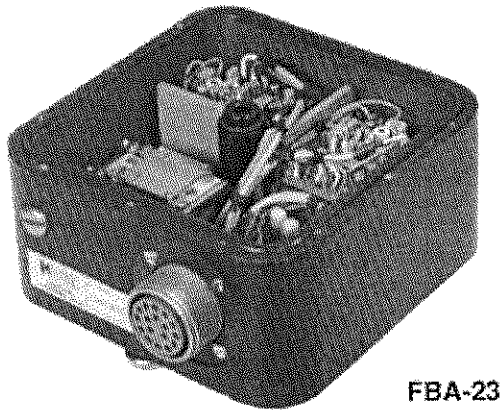

Figure 2-10. Accelerometer Model FBA-23

2.5. Damage

2.5.1. San Fernando Earthquake (1971)

Ventura (1994) describes the previous damage caused by the 1971 San Fernando earthquake in the target structure. He states that all of the columns located at the corners suffered structural damage. In addition some exterior girders in exterior frames in the second floor were cracked and one shear wall in one sublevel had a small diagonal crack. Ventura emphasizes that cracking in columns was near the spandrels in the second floor. The repairs for the damage on the second floor consisted of stiffening the joint between the columns and girders using post-tensioned tendons.

2.5.2. Northridge Earthquake

After the Northridge earthquake in 1994, the structure showed similar damage. Naeim (2000) gives specific information about the damage suffered by the target structure and classified the general damage on the structure as moderate. Specifically he states that there was some damage in girder-column connections as well as multiple cracks in the reinforced concrete components of the lateral force-resisting system. However, the mechanical equipment and pipes in the second sublevel and roof behaved extremely well because no apparent damage was observed. The adjacent parking facility did not survive the earthquake, although the main structure did not show any sign of tilting. The cracks in the sublevels and second floor were repaired with epoxy injection. Details of damage and repairs are shown in Figure 2-11 to Figure 2-14.

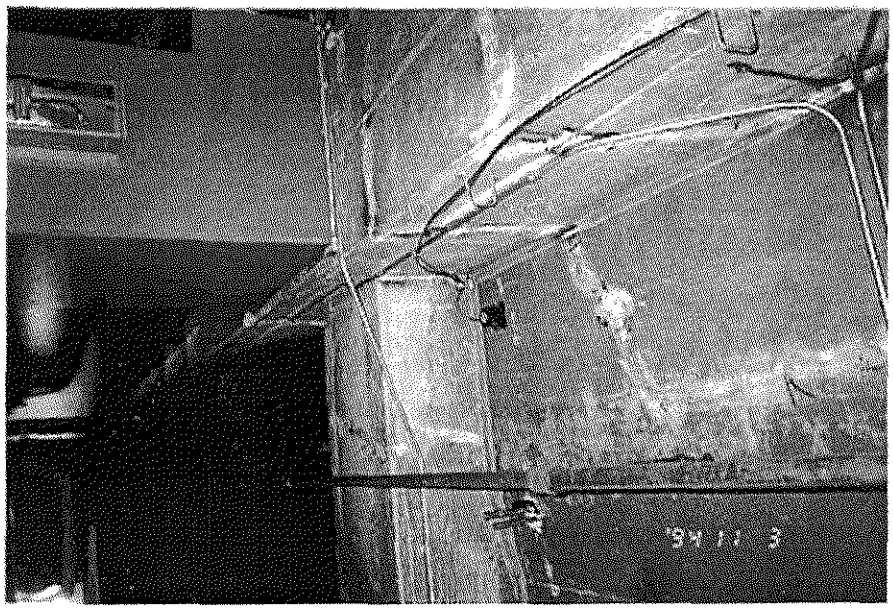

Figure 2-11. Damage to girder, column and wall (Repaired with epoxy) (Naeim, 2000)

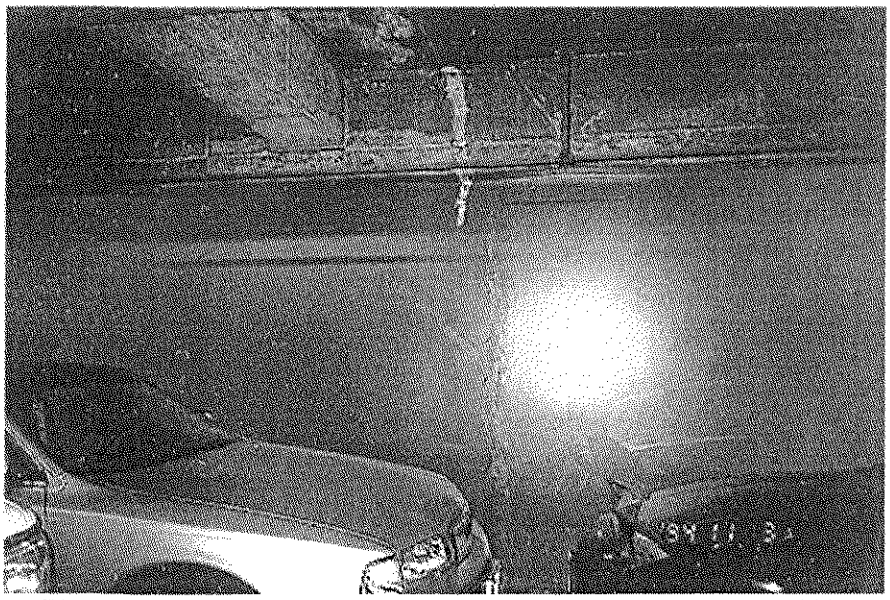

Figure 2-12. Wall after painted and repaired with epoxy (Naeim, 2000)

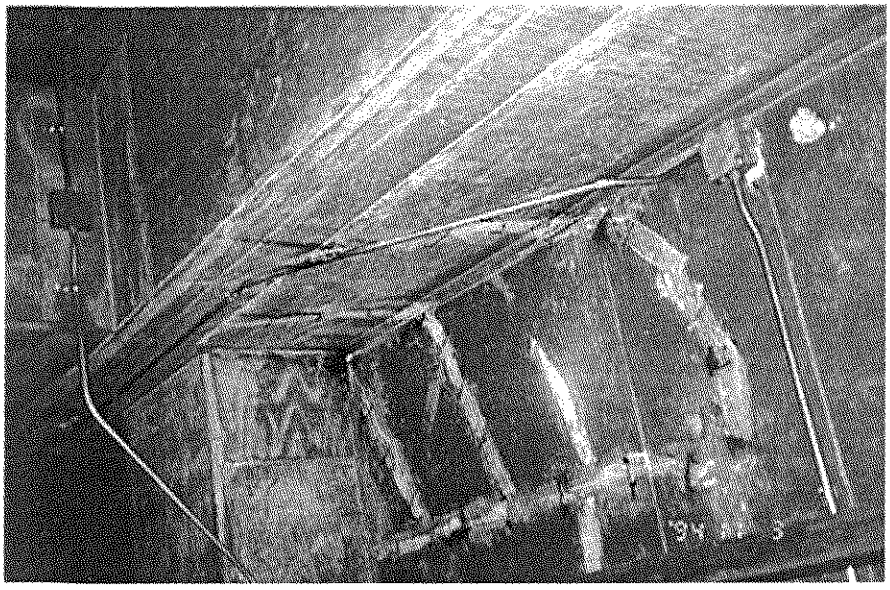

Figure 2-13. Epoxy repaired cracks in shear wall (Naiem, 2000)

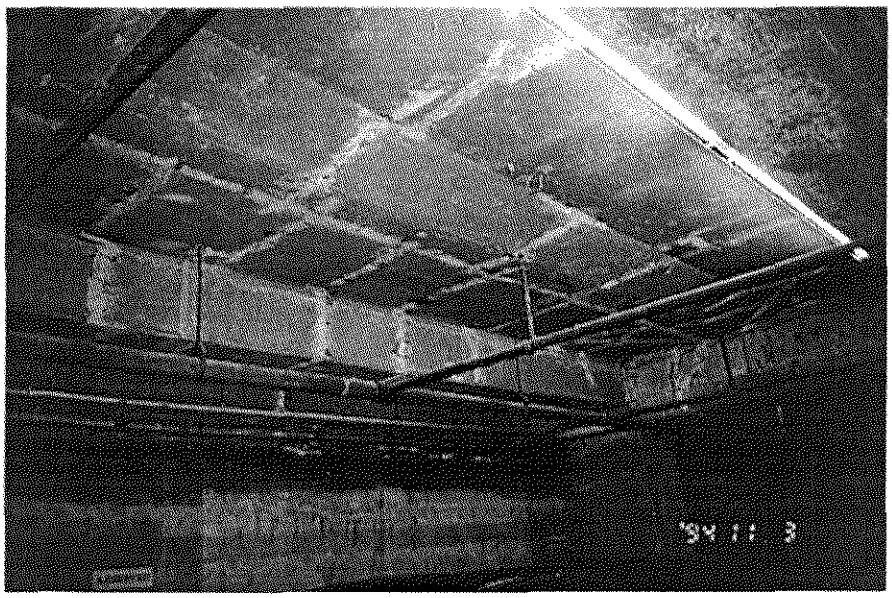

Figure 2-14. Epoxy repaired cracks on slab and beam (Naiem, 2000)

3. Model Description

3.1. Introduction

This chapter describes the nonlinear analysis routine, the models used to represent the material properties as well as the developed models of the target structure. The results for the different building models are compared and discussed.

3.2. Nonlinear Analysis Routine

LARZ was the software used to calculate the nonlinear response for the target structure. This program was developed at the University of Illinois by Otani (1974) and modified later by Saiidi (1979) and Lopez (1988).

The numerical analysis used in LARZ is based upon some assumptions:

1. LARZ was developed to analyze two dimensional (2D) models. All the input and output data is defined in one plane. The displacements for each degree of freedom (DOF) are defined in the horizontal plane and the rotations are about an axis perpendicular to the plane of the model (Figure 3-1).
2. The structural members are assumed to have no mass and are divided into three sections. The sections include rigid lengths at the supports, nonlinear flexural springs at the end of the rigid length, and a linear elastic portion between these springs(Figure 3-1).
3. The members are oriented along their centroidal axis.

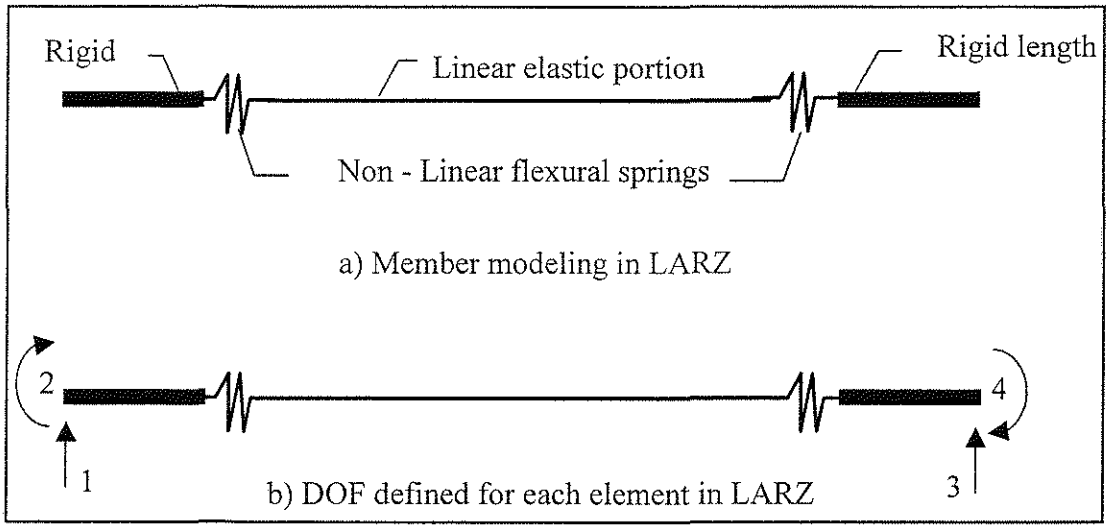

Figure 3-1. Element Modeling and DOF

4. Input accelerations are applied to the base of the structure in one horizontal direction.
5. Columns at the base are connected to a infinitely rigid foundation.
6. A horizontal single DOF is defined for each floor.
7. Each DOF has a lumped mass.
8. Changes in the length of members are neglected.
9. Joint cores at connections are considered to be infinitely rigid.
10. The nonlinear responses of girders and columns are in flexure only and hysteresis is defined by Takeda (1970) rules.
11. The nonlinear response for walls encompasses flexure and shear. Hysteresis for flexure is defined the same as for girders and columns (section 3.3.1). Shear deformations are defined with a similar relationship but with simplified rules, as describe in section 3.3.2.

12. Gravity effects (P-Δ) may be taken into account.

13. Slip of reinforcement may be included at connections (girder-column).

Two types of nonlinear analyses were calculated for the target structure: static and dynamic. The nonlinear static analysis (NLSA) was used to calculate the base shear response and the estimated yielding mechanism. The nonlinear dynamic analysis (NLDA) was used to calculate the lateral drift of the model and compare it with the recorded response.

Gravity effects or P-Δ effects, were taken into account in the analyses. LARZ accommodates second-order effects by softening the stiffness matrix, which results in larger lateral displacements.

The equivalent viscous damping in the modeled system was assumed to be 2% of the critical damping. LARZ assumes that the damping matrix is a linear combination of the mass and structural stiffness matrix, represented as:

$$[C] = \alpha[M] + \beta[K] \tag{3.1}$$

where:

[C] = damping matrix at each time step

α = constant

[M] = mass matrix

β = constant

[K] = stiffness matrix at each time step

The variables α and β were calculated according to the following equations:

$$\xi_1 = \frac{1}{2\omega_1}\left(\alpha + \beta\omega_1^2\right) \tag{3.2}$$

$$\xi_2 = \frac{1}{2\omega_2}\left(\alpha + \beta\omega_2^2\right) \tag{3.3}$$

Where:

ξ_1 = coefficient of damping for first mode = 0.02

ω_1 = circular frequency for first mode

ξ_2 = coefficient of damping for second mode = 0.02

ω_2 = circular frequency for second mode

The values of ω_1 and ω_2 were calculated and used to estimate the values for α and β.

3.3. Member properties

3.3.1. Girders and Columns

In order to calculate the flexural deformations of the structural elements, the moment-curvature (M-ϕ) relationship for each element was calculated and provided as an input. The M-ϕ relationship is a trilinear relationship defined by distinct points representing: cracking, yielding and ultimate moment-curvature values (Figure 3-2).

The stages defined by the values shown in the graph are the cracking in the concrete (ϕ_{cr},M_{cr}) and the yielding in the steel (ϕ_y,M_y). A post-yielding slope of 1% of the slope to yield was used to define the third portion of the M-ϕ relationship.

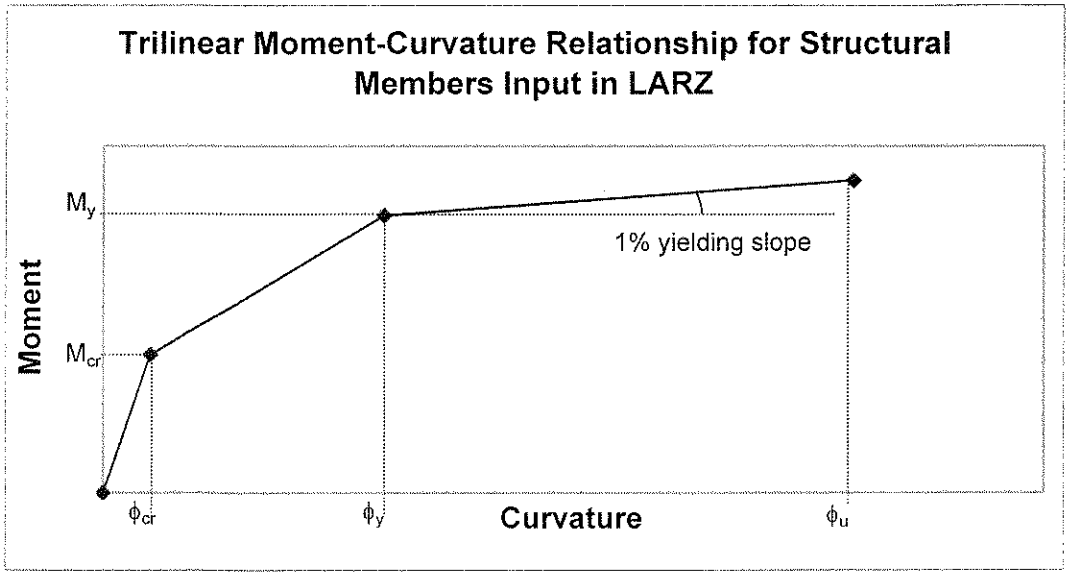

Figure 3-2. Trilinear Moment-Curvature Relationship

The M-ϕ relationship shown in Figure 3-2 was calculated assuming:

- The idealized concrete stress-strain model by Hognestad (1951) was used.(Figure 3-3)
- An elasto-plastic behavior was assumed for the reinforcing steel. (Figure 3-4)
- The axial load in columns acted in the geometric center of the element and its value was the corresponding load for the tributary area.
- The tensile stress in the concrete was neglected.

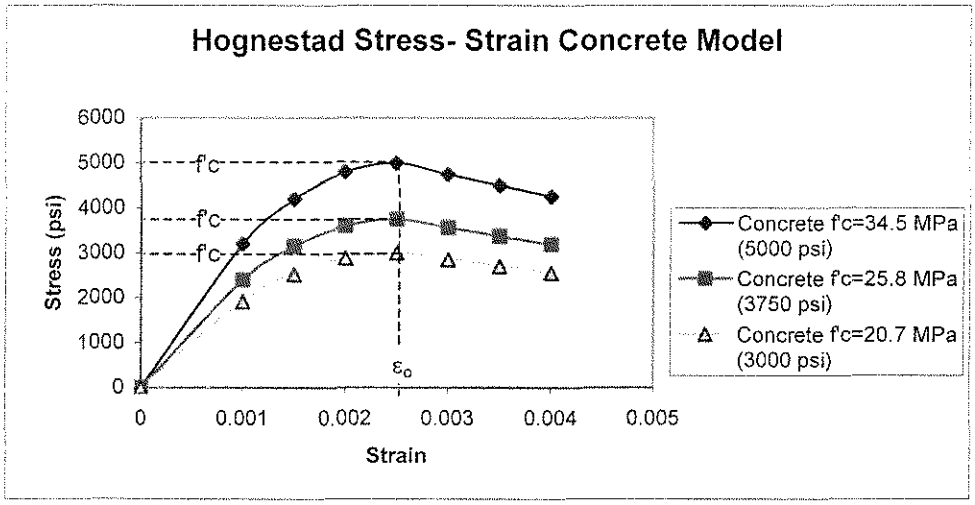

Figure 3-3. Hognestad Concrete Model

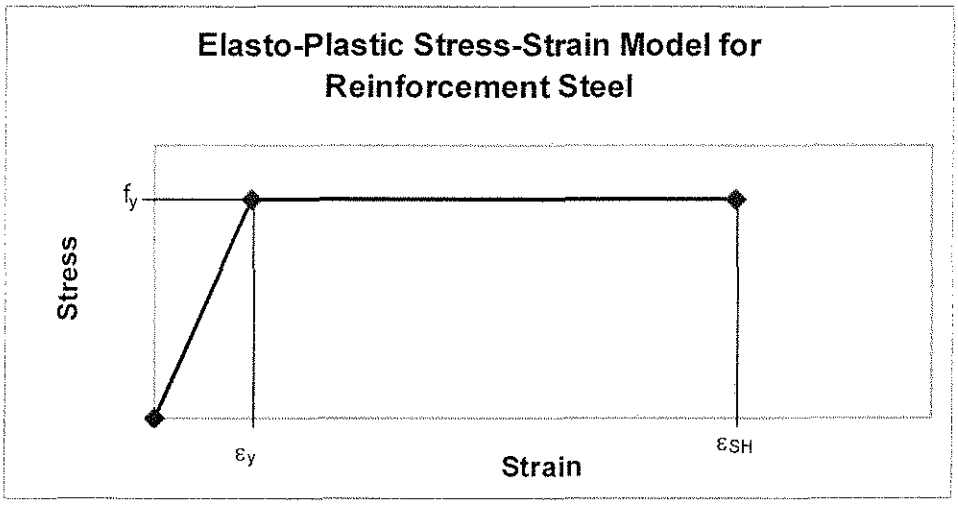

Figure 3-4. Elasto-Plastic Curve for Steel

The gross sectional area was used to calculate the initial stiffness for each element. The stiffness calculated for the girders includes a slab contribution as shown in Figure 3-5 and Figure 3-6.

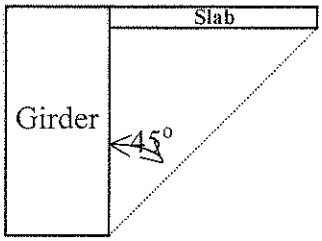

Figure 3-5. Slab Contribution to Exterior Girder.

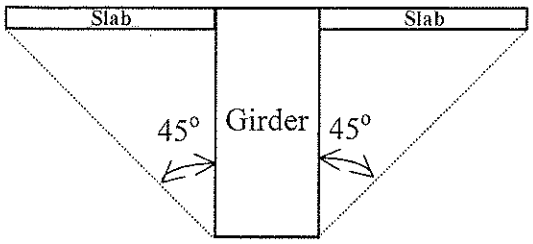

Figure 3-6. Slab Contribution to Interior Girder.

The M-ϕ relationship was affected by the rotation due to slip of the reinforcement at the joints. This relative movement between the concrete and the reinforcing steel was calculated assuming that:

- No pullout will occur. The anchorage length provided is sufficient to prevent such effect.
- The tensile stress in the reinforcement induces a linear variation on the moment.
- The angle of rotation was measured with respect to the centroid of compression reinforcement.

- Bond stress was uniformly distributed along the anchorage length with a value of $6\sqrt{f'c}$.
- The steel reinforcement reached yielding.

3.3.2. Walls

Walls were modeled in LARZ as shown in (Figure 3-7). Each segment has two degrees of freedom (DOF). All the walls were modeled with 10 subelements.

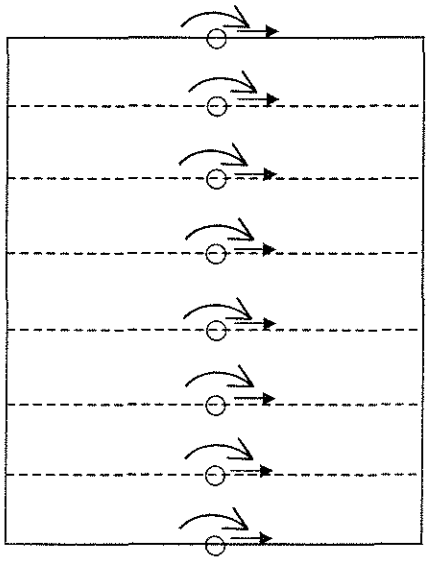

Figure 3-7. Wall Subdivisions and DOF

The flexural capacity and stiffness of the walls were calculated based on the data in structural plans and using the same procedure as for columns and girders that was explained in Section 3.2.1. Shear hysteresis for the walls was modeled as shown in (Figure 3-8). This model was developed by Lopez (1988). Shear values at cracking and yielding were defined as:

$$V_{cr} = 4\sqrt{f'c} \qquad \text{(psi)} \tag{3.4}$$

$$V_y = \rho \cdot fy \qquad \text{(psi)} \tag{3.5}$$

where:

V_{cr} : Shear force at cracking

f'c : Concrete compressive strength

V_y : Shear force at yielding

ρ : Wall transverse reinforcement ratio.

fy : Yielding stress for steel

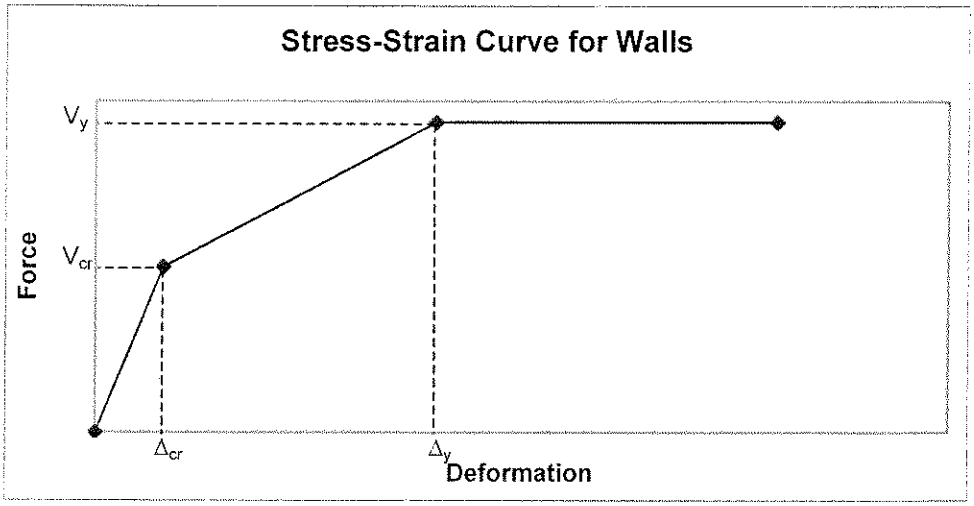

Figure 3-8. Stress Strain Model for Walls

Rotation of the reinforcement was not taken into account for the analysis of the walls.

3.4. Representation of the Target Structure

3.4.1. Selected frames and properties

The target structure was modeled as two main frames (2nd sublevel to roof) and a wall frame (2nd sublevel to ground). Only two of the three main frames were modeled because the exterior frames were nearly identical with only few differences in some members in the sublevels. Differences in the exterior frames were noted in all the girders in the ground level and first sublevel as well as in one of the interior

columns. The differences were in reinforcement ratio. The moment curvature values of these elements were averaged and included in the modeled frame.

To compare the behavior of the model with the behavior of the instrumented structure, a non-linear dynamic analysis was completed. The input earthquake motion used for the analysis was the acceleration record obtained from the building instrumentation on channel 13 (Figure 2-9). That was the accelerometer located in the chosen modeling direction.

An estimate of the lateral stiffness of each frame was calculated to determine an appropriate distribution of mass for the modeled frames. Each frame was modeled separately using (as described in Section 3.2) and subjected to increasing lateral loads to calculate a force-deformation relationship for the frames (Figure 3-9). The lateral load distribution increased linearly with height.

As can be seen in Figure 3-9 the exterior frame has a stiffness of approximately 2/3 the stiffness of the interior frame. The percentage of the total building weight assigned to the modeled frames was calculated as shown below:

$$\frac{\frac{2}{3}K_{int} + K_{int}}{2 \cdot \frac{2}{3}K_{int} + K_{int}} = \frac{5}{7} = 0.71$$

Consequently, 71% of the total weight of the building was used in the analysis of the model.

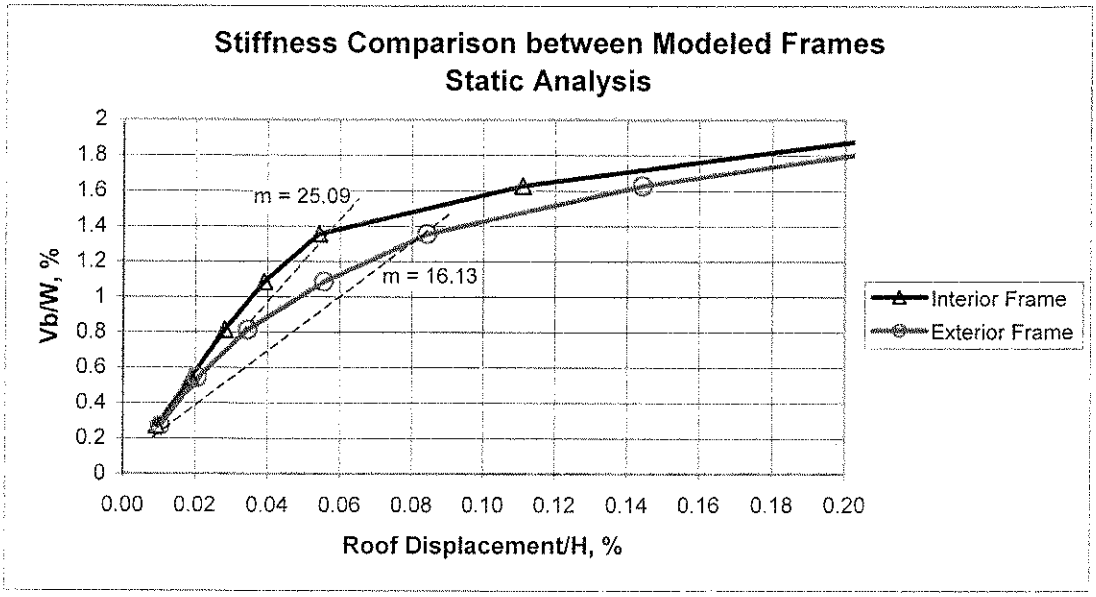

Figure 3-9. Frame Stiffness

The recorded response of the building indicated that the deformations in the sublevel were not significant at the time of maximum drift (Figure 3-10). The maximum drift distribution over the two sublevels was shown to be 0.9 in., or 0.4% of the total height of the sublevels, at a time of 5.84 sec (Figure 3-11). It appears as though the embedment provided by the soil was enough to restrain the response of the sublevels to small levels. Therefore, two models were completed to investigate the behavior of the building: 1) a model including the floors above the ground level, and 2) a model including all floors and sublevels.

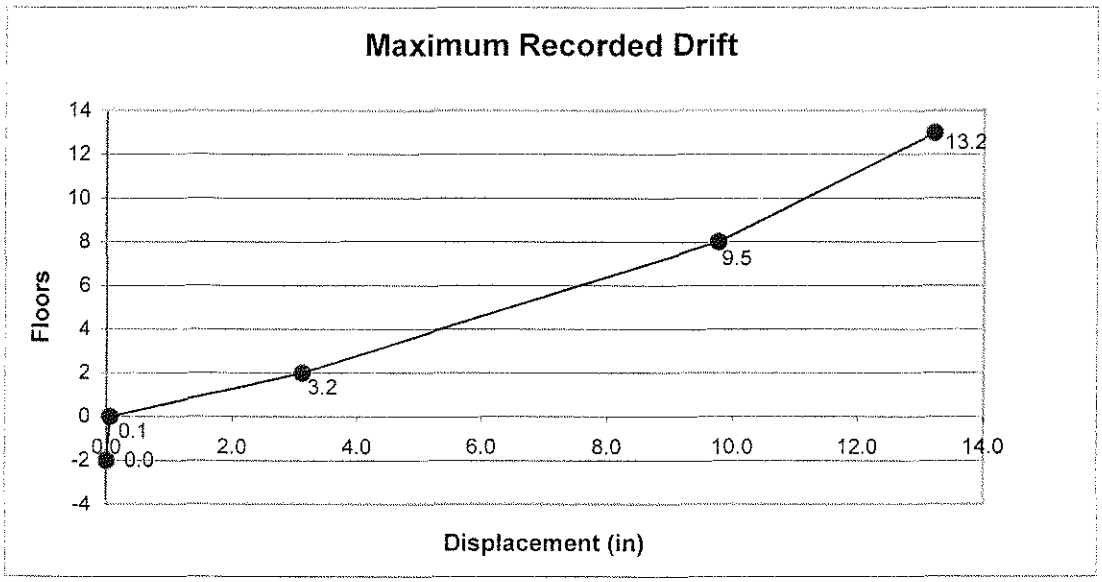

Figure 3-10. Maximum Recorded Drift

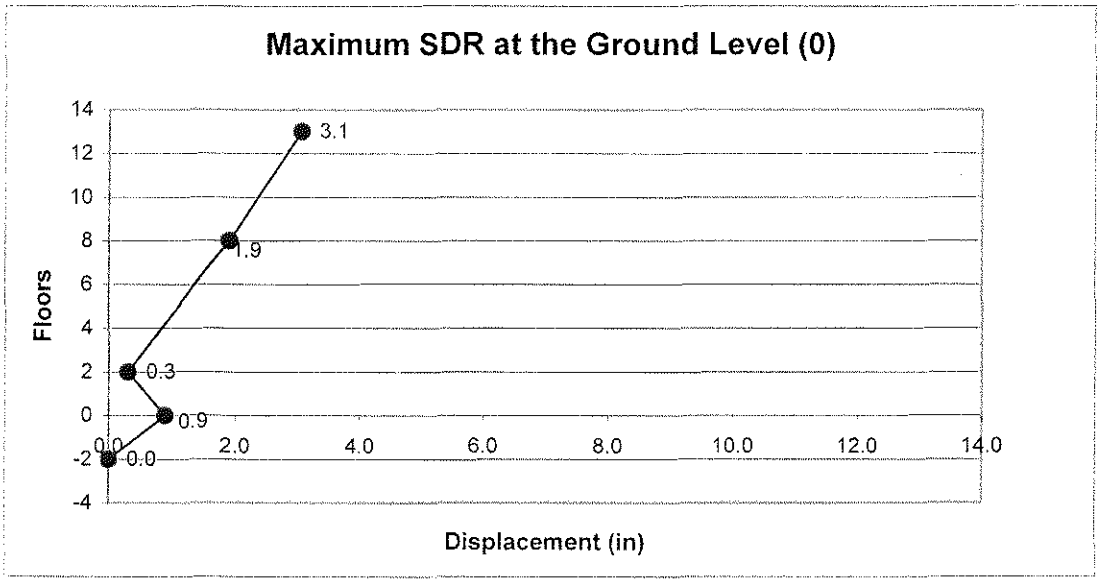

Figure 3-11. Maximum SDR at the Ground Level

There were several challenges during the process of modeling the sublevels. One of the biggest challenges was the modeling of the walls as a separate frame. The wall frame was modeled as a one-bay frame with a wall member, a column element

and a girder connecting the two vertical elements. Girder and column properties were decreased until these elements carried nearly zero load during the response. In the next section the results for this model will be shown and discussed.

3.4.2. Results

3.4.2.1. Model without sublevels

For the first model (Model A), the building was modeled using the 13 floors above ground and with a fixed foundation at the ground level. This model was developed and compared with the second model to determine how the modeling of the foundation affects the overall response of the structure.

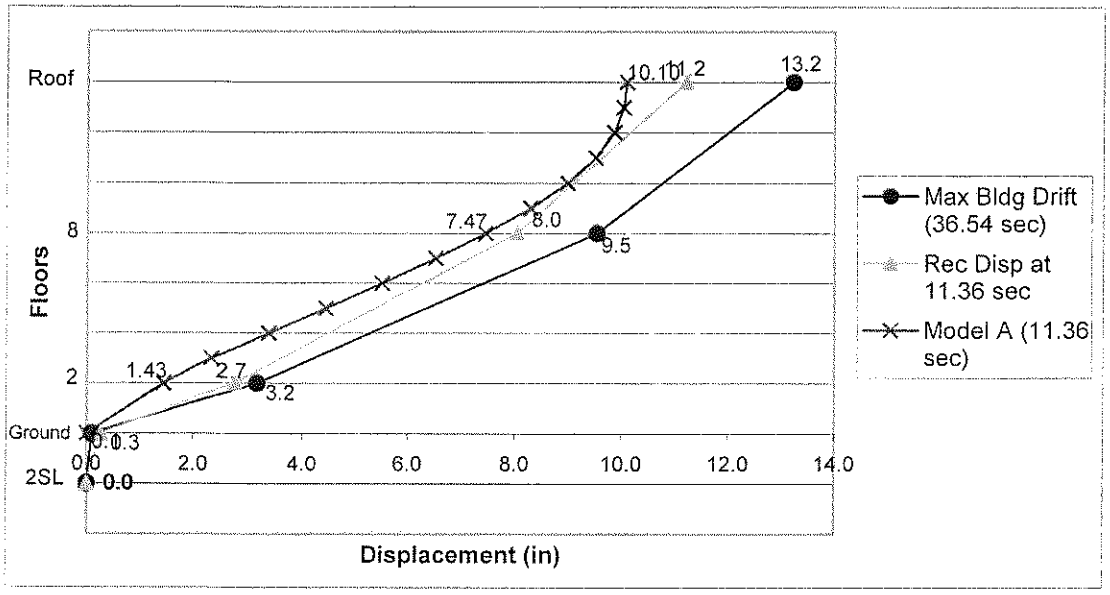

Figure 3-12. Comparison of Response for Model A (without Sublevels)

The deformed shapes are shown in Figure 3-12 for the model with the recorded response at two different times. The first recorded deformed shape is for the time of maximum displacement at the roof (36.54 sec). The second recorded deformed shape is for the time of maximum displacement calculated in the model that

occurred at 11.36 sec. The response of the model cannot be compared with the maximum recorded response (36.54 sec) because it occurs at a different time, however the maximum recorded response will be used as an upper limit. It can be seen that because this model is fixed at the ground level the displacement at the second floor is not as large as it was recorded. It keeps having a much less displacement value than the recorded displacement value through the eighth floor, after that level the displacements are amplified. However the deformed shapes of the record and the model are very alike, this shows how the overall response has been well represented.

The maximum recorded displacement occurred at 36.54 sec, while in the model the maximum displacement occurred at 11.36 sec. A fast Fourier transform (FFT) was done for the acceleration input (Ch. 10) to evaluate if there was a considerable contribution for the natural frequencies of the building in the time range between 20-40 sec where the maximum recorded displacement occurred (Figure 3-13&Figure 3-14). As the graphs show, most of the energy was released during the first 20 seconds of the earthquake.

The amplitude for the first natural frequency (0.88 hz, T = 1.14 sec) of the structure in Figure 3-13 is almost three and a half times the amplitude for the same frequency in Figure 3-14. The amplitude value for the second natural frequency (2.53 hz) for the first range of time (0-20 sec) was eight times bigger than for the second range of time (20-40 sec). These values confirm that most of the energy was released during the first twenty seconds of the earthquake, where the acceleration peak is

located. A large amplification of response would not be expected for a structure with a frequency of 0.88 hz in the second range of time (20-40 sec).

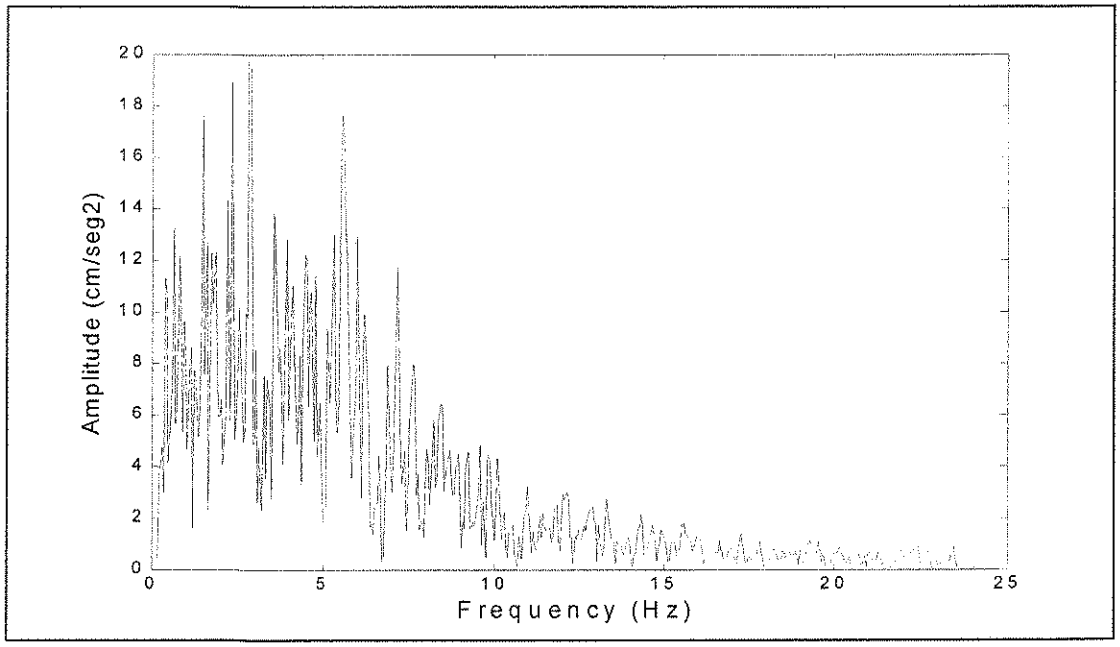

Figure 3-13. Fast Fourier Transform for Acc. Input (Ch. 10) 0-20 sec

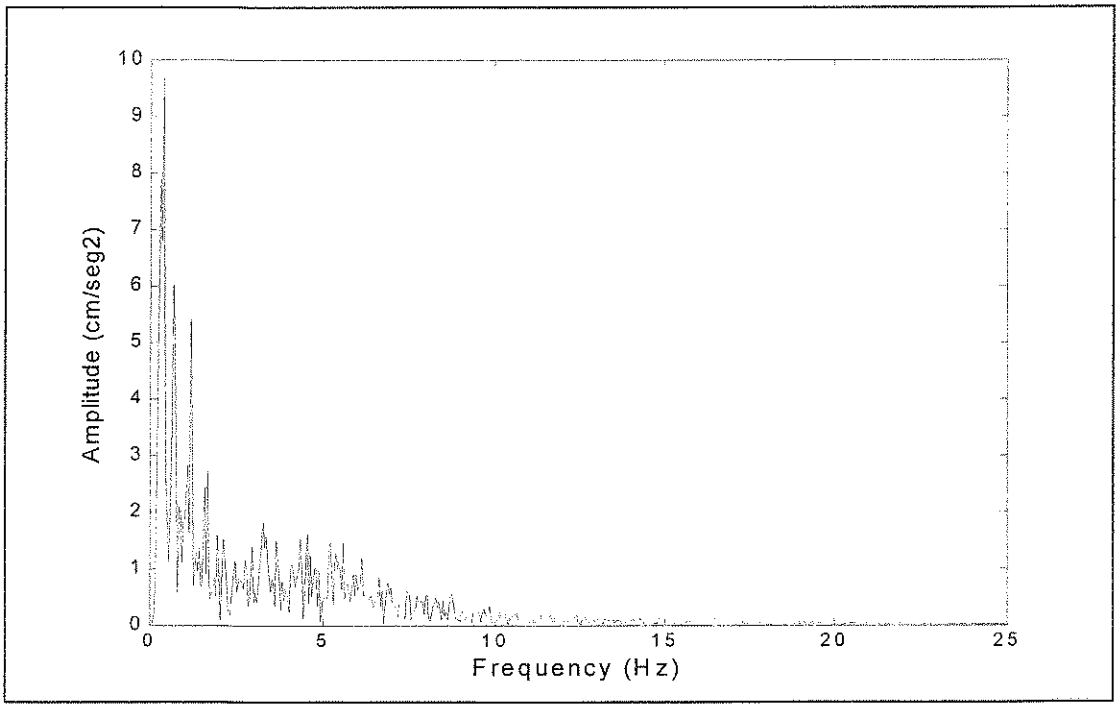

Figure 3-14. Fast Fourier Transform for Acc Input (Ch. 10) 20 - 40 sec

It is important to remember that the period of the structure will soften during response to the earthquake. During the latter stage of the earthquake the structure becomes more vulnerable to higher period excitations. A reasonable value for the new effective period may vary from 2 – 4 times the initial period (T_o). For this building, an effective period of $2T_o$ would be 2.3 sec (0.44 hz). Figure 3-14 shows a peak around 0.4 hz (2.5 sec), which may contribute to the larger recorded response during the time range of 20 to 40 sec.

The long period motion noted in the base acceleration records (Figure 3-22, 31 sec – 36 sec) appears unusual in the initial evaluation of the building response. However, the response of the structure at the roof corresponds to this long period motion and may represent a resonant response of the building to basin motion recorded in this time range (USGS).

3.4.2.2. Model including sublevels.

The second model (Model B) included all floors and sublevels. The response for this model is shown in Figure 3-15.

The results indicate that the foundation of the model is stiff compared to the actual foundation. It was necessary to change the sublevel characteristics to simulate a softer foundation. LARZ does not easily allow modeling of the soil properties, consequently it was necessary to change the structural properties of the walls to provide a more flexible response at the sublevels (Model C, discussed in section 3.5.1). The displacement history for models A and B is shown in Figure 3-20 and Figure 3-21.

A FFT was developed for the acceleration input used to analyze Model B (Ch. 13). Figure 3-16 & Figure 3-17 show the results for two periods of time. The results did not change in comparison with what was obtained for the accelerations from Ch. 10 (Figure 3-13 and Figure 3-14). Most of the energy was released in the first 20 seconds of the earthquake.

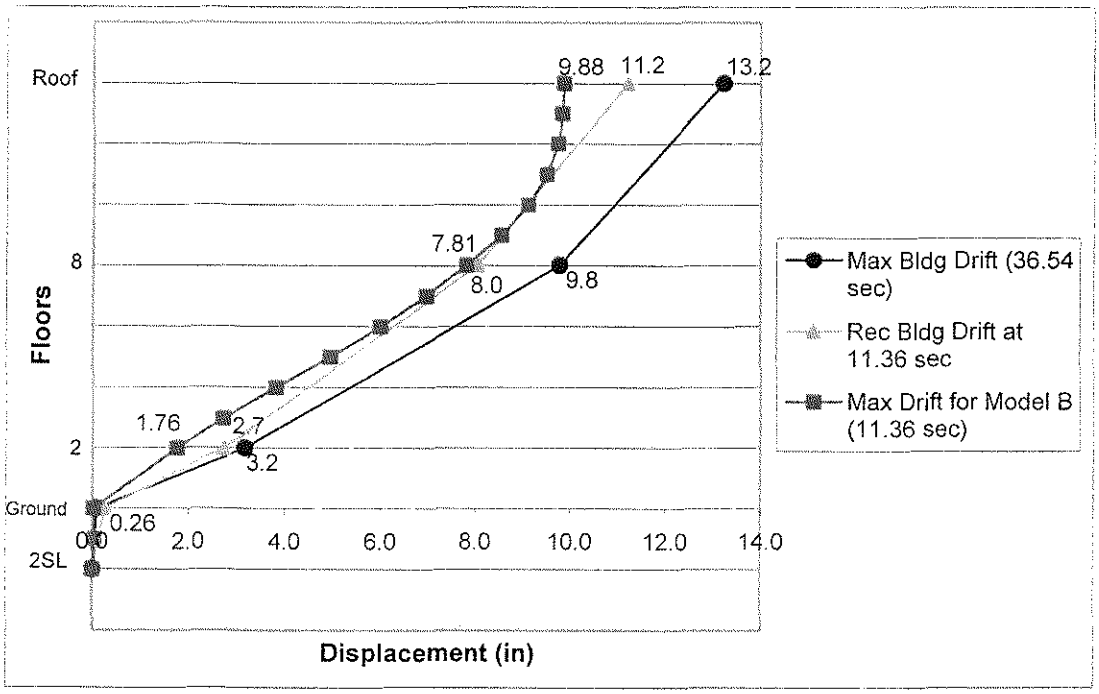

Figure 3-15. Deformed Shape for Model B

Comparing Figure 3-16 and Figure 3-17 is observed that the amplitudes for the first two natural frequencies of the building are larger for the time range of 0 – 20 sec. The amplitude value for the first natural frequency (0.57 hz) is 4.5 times larger than the amplitude value for the period between 20-40 sec. The second natural frequency (1.9 hz) had an amplitude almost eight times larger for the first range of time compared to the second range of time.

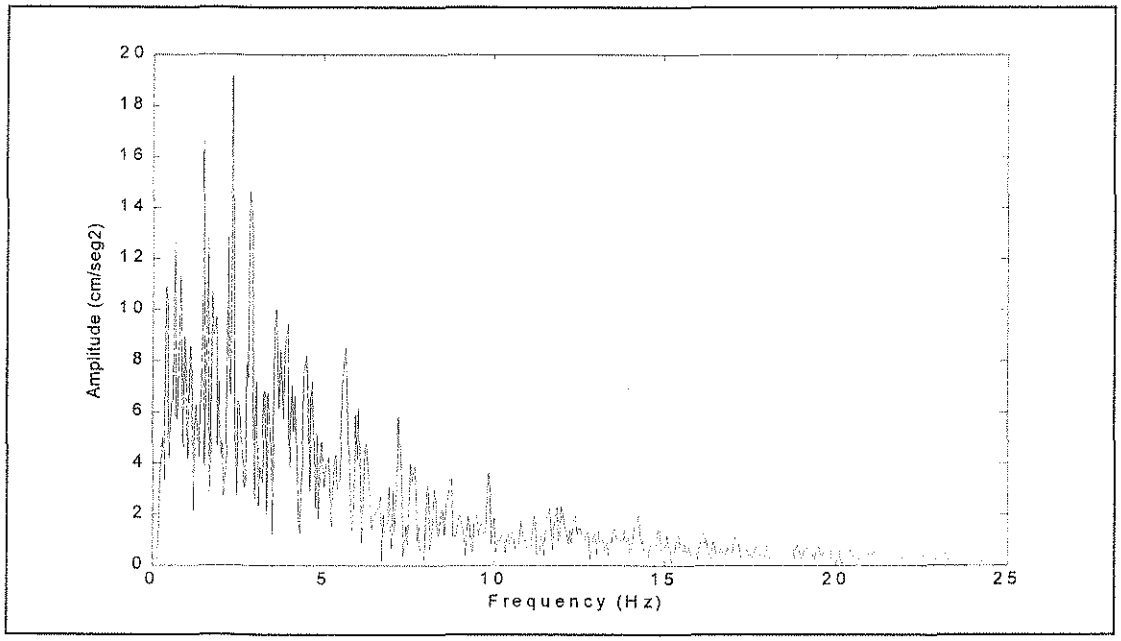

Figure 3-16. Fast Fourier Transform for Acc Input (Ch. 13) 0 - 20 sec

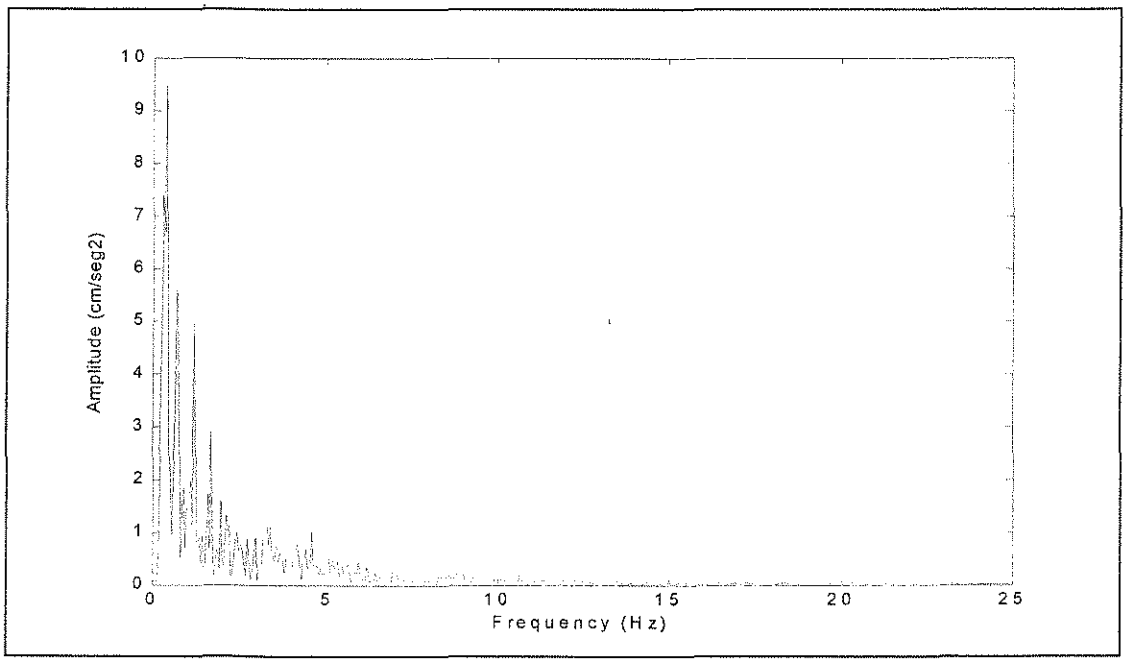

Figure 3-17. Fast Fourier Transform for Acc Input (Ch. 13) 20 - 40 sec

When the displacement record for the ground level and second floor are compared, the time of maximum displacement shifts from 5.86 sec. for the ground level to 35.02 sec for the second floor. At the ground level the maximum displacement was 0.9 in, and at the second floor the value was 3.23 in. The maximum displacement at the second floor was nearly ten times that recorded at the same time for the ground level [over a height of 7 m (23 ft)]. At the second floor, the displacements are much larger and the time ranges at which they occur are different than the response at the ground level. In comparison, the amplification of the displacement response from the second floor to the roof at the time of 35.02 sec. [over a height of 43 m (141 ft)] is only approximately a factor of 3.5. Therefore, the first story undergoes a drift of 1.2% of the story height (3.3 in.), and the remaining portion of the superstructure (12 stories) undergoes a drift of only 0.6% of the total height (9.9 in.) at that time of 35.02 sec. At the time of maximum roof drift (36.54 sec), the drift for the first level was 1.11% of the story height (3.1 in.) and the drift for the floors 2-12 was 0.61 % of its height (10.1in.).

The comparison of the response at the ground level and second floor (Figure 3-18 and Figure 3-19) shows how the displacement frequencies and amplitudes are modified through the building. The high frequencies in the ground level motion (first 20 seconds) are greatly reduced in the response shown for the second floor. In addition, the low frequency response in the later portion of the record (20-40 sec) is highly amplified.

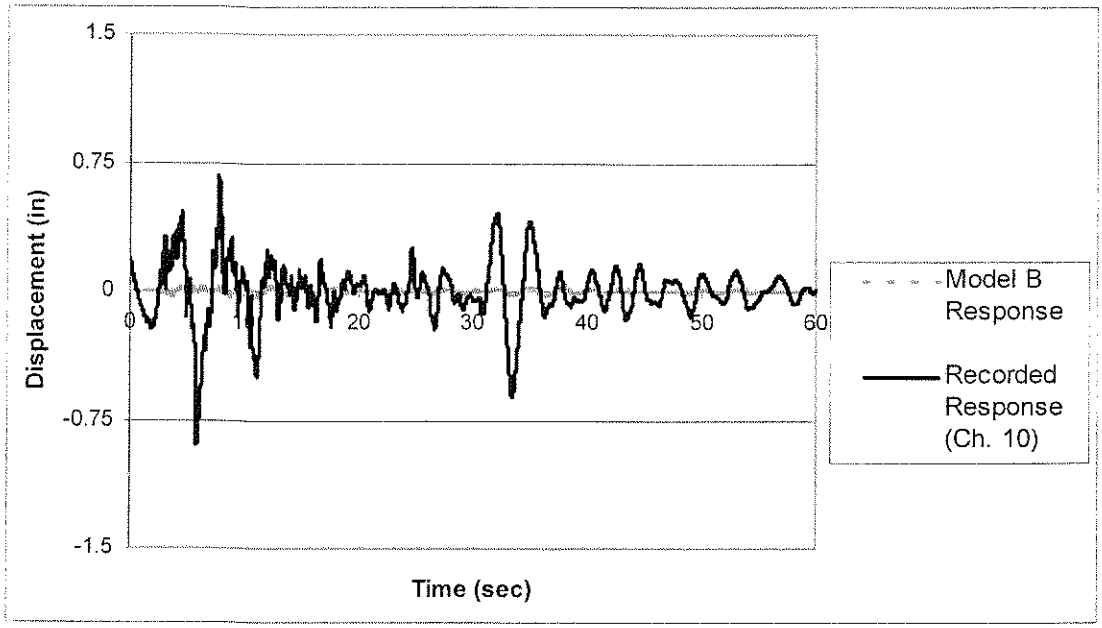

Figure 3-18. Displacement History at Ground Level

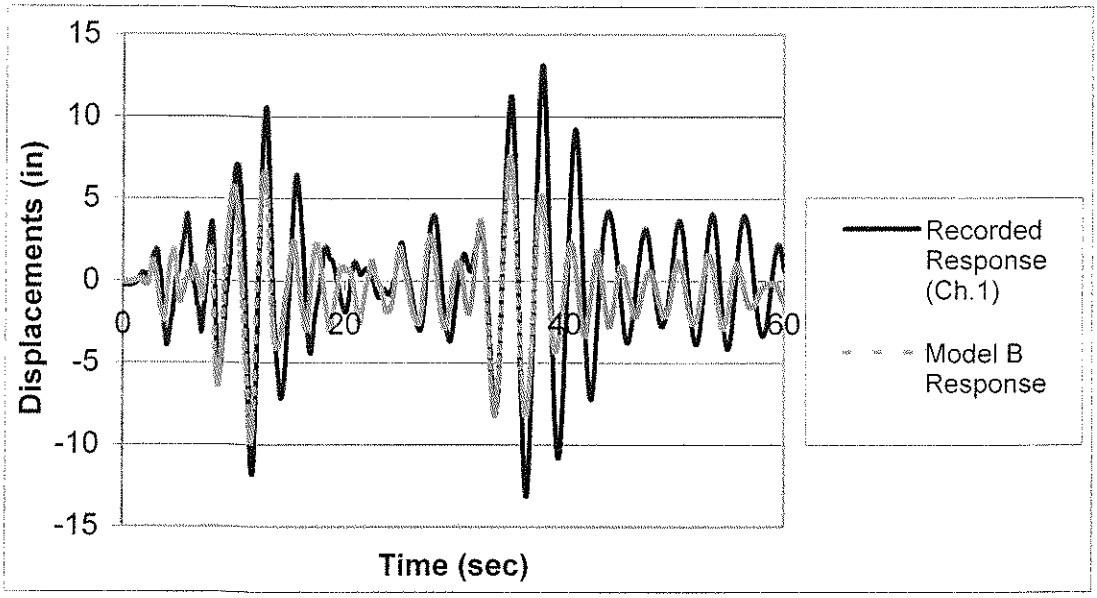

Figure 3-19. Displacement History at 2nd Floor

In Figure 3-20 and Figure 3-21, the periodicity of the modeled response compares relatively well with the recorded response except during two ranges of time. Between 16 and 24 sec, the models appear to have a shorter period of response

than the actual building for that range of time. Between 40 and 50 sec there is a small shift in the displacement axis of approximately 0.3 in. for model A, and approximately 0.7 in. for model B. For models A and B the permanent deformation occurred at the fourth level. At approximately 40 sec of response, models A and B appear unable to simulate the magnitude and periodicity of response recorded in the actual structure. This occurs close to the time of maximum response for the actual building.

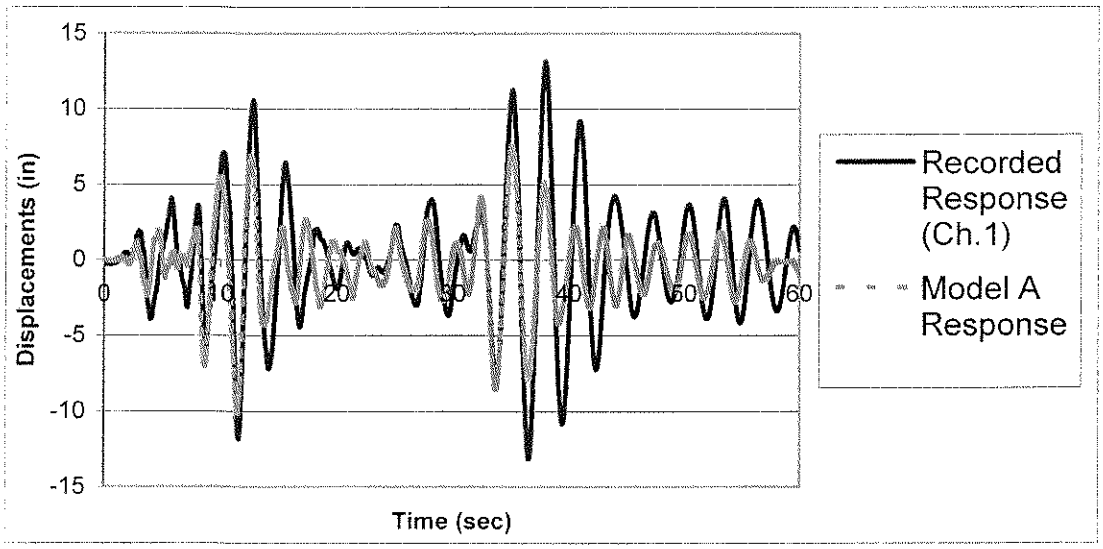

Figure 3-20. Displacement History at Roof for Model A

Figure 3-22 shows the acceleration record at the base of the structure (Ch. 13), which was the acceleration input used to analyze the models. The maximum displacement response of Model B occurs at 7.66 sec., but the actual structure has the maximum displacement response at 36.54 sec., apparently excited by the low amplitude accelerations present in the record between 32 – 36 sec. The maximum

displacement recorded at 36.54 sec could be attributed to the large amplification in the first tall story as discussed before.

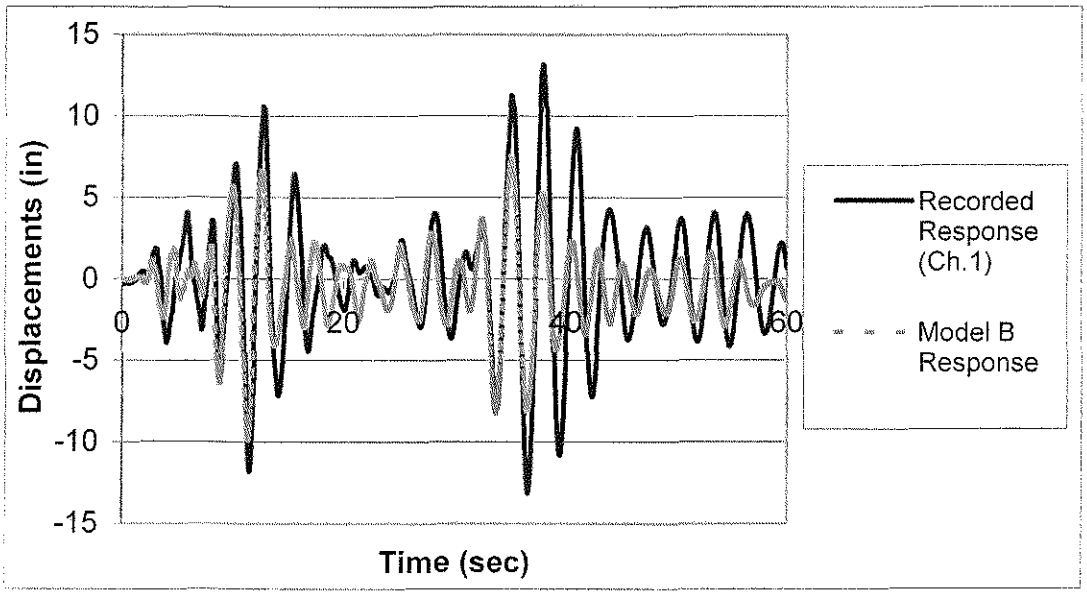

Figure 3-21. Displacement History at Roof Model B

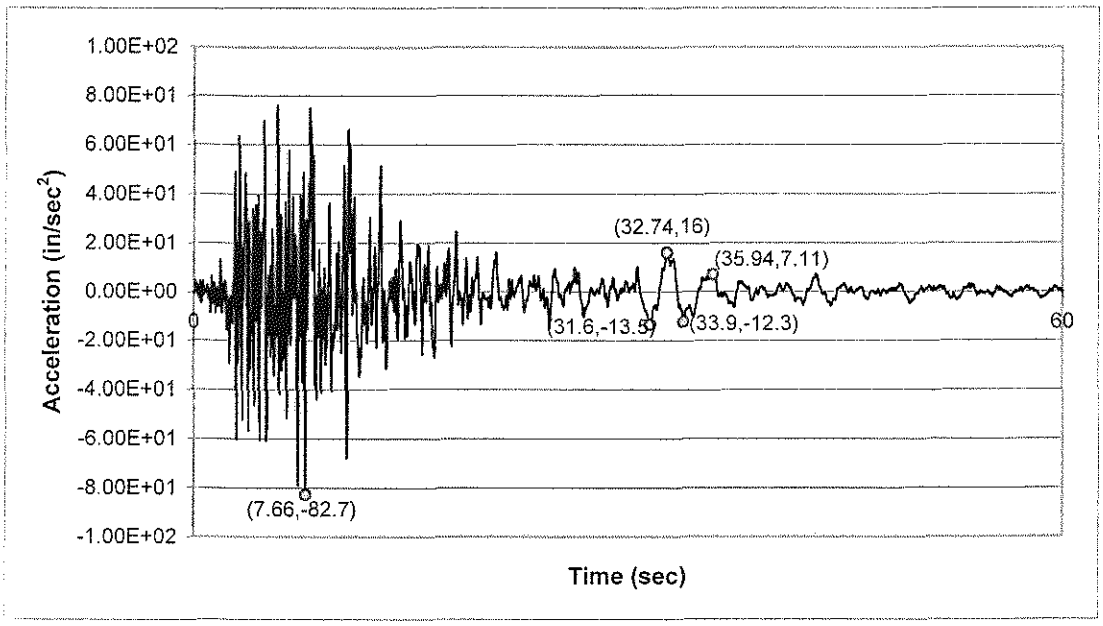

Figure 3-22. Acceleration Input (Ch. 13)

3.5. Modified Properties

Properties for girders and walls were modified in Model C to investigate means for amplifying the lateral response. This model is discussed in the next section.

3.5.1. Modified Walls and Sublevels

The target structure has a pile foundation. Soil interaction for pile foundations is very complex and may be analyzed including soil-pile interaction, effects of the pile cap, non-linear soil response, etc. There are many different approaches to solve for the dynamic response of pile foundations. The dynamic behavior of piles groups is very different than single pile dynamic behavior. Consequently, methods to solve for a single pile are not applicable to a group of piles.

Finn et al (1997) developed a non-linear analysis procedure for pile groups. In their paper they show how the weight of the superstructure affects the response of the pile foundation. The inclusion of the weight of the superstructure reduces the stiffness of the foundation, which will produce more displacement of the structure. When the weight of the superstructure was included in the analysis of the foundation its stiffness changed between 50% and 70%.

Modifications were made to the wall and girders in the sublevels, to represent the increased response (less stiff response) noted in the actual structure. As a consequence of the modification, the overall response over the height of the building was affected as described below.

For Model C, the moment of inertia of the wall was reduced to represent the reduction of stiffness produced by the weight of the superstructure and the previous damage of the structure in 1971 (section 2.5.1), the M-ϕ relationship for the girders in the sublevels was assumed to be bilinear ($M_{cr} = 0$), in addition to the modified wall properties.

Han and Cathro (1997) showed the modeling of the foundation can change the response of a tall building with pile foundation substantially. The maximum peak displacement is reduced if a rigid base is used instead of modeling the actual piles. The periodicity of the structure, accounting a softer foundation, is lengthen.

The percentage of reduction of stiffness for the wall, from Model B, was 82.5%. This number came from a combination of the values suggested in FEMA 273 and Finn et al (1997). FEMA 273 guidelines recommend using 50 % of the uncracked stiffness for walls with cracks. The damage report after the San Fernando earthquake stated that there were some cracks in the walls and the stiffness was reduced by 50 % for the model. To account for the foundation effect as describe by Finn et al (1997) the properties still should be decreased additionally by 50 – 70%. A more reasonable value of 35% (half of the maximum suggested value) was selected to be used in conjunction with the previous 50% reduction. The combination of these percentages gives a reduction of 82.5%.

3.5.1.1. Results

The results improved substantially in the sublevels using Model C. The deformed shape and the displacement history follow the record very closely. The results are shown in Figure 3-23 and Figure 3-24.

As can be seen in Figure 3-24, the periodicity of the model is nearly the same as the periodicity of the record. This confirms that the flexibility of the sublevels has a big impact in the response of the structure.

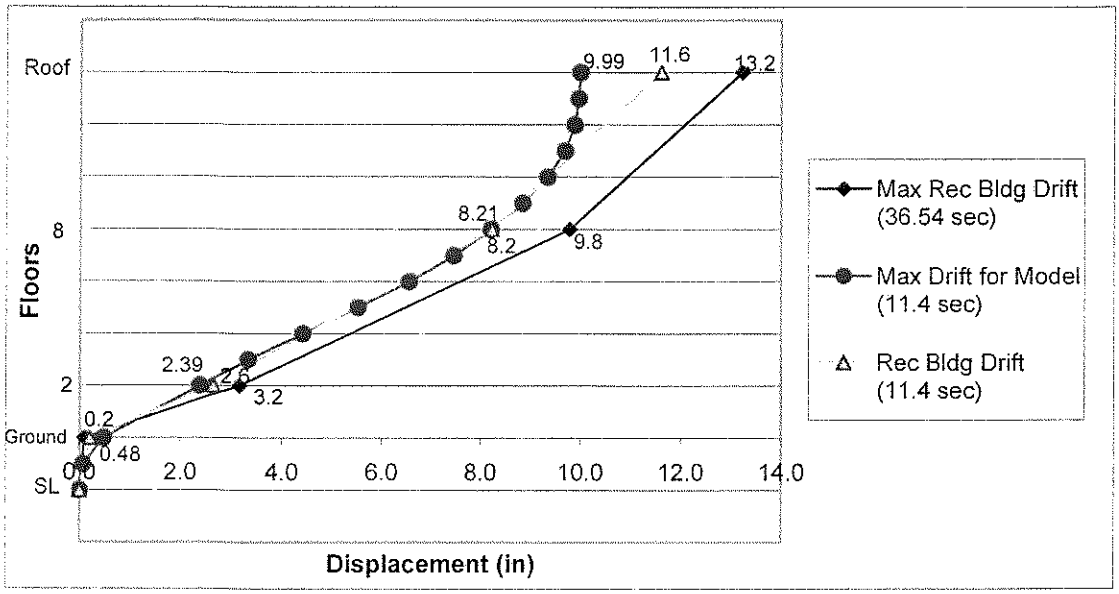

Figure 3-23. Deformed Shape for Model C

The results for Model C (Figure 3-23 and Figure 3-24) show the improvement in the deformed shape and the periodicity compared to the recorded response. Model B (Figure 3-21) has 4 ranges of time in the displacement history that did not follow the periodicity of the record, those times were: 14.8 – 24.6 sec, 30-32 sec, 40-50 sec, 53.3-60 sec. Model C shows an improvement in those ranges as it only

showed 3 shorter ranges of time that did not follow the periodicity. The time ranges with a poor comparison to the record were: 17-24.5 sec, 41.3-48.2 sec, 56-60 sec.

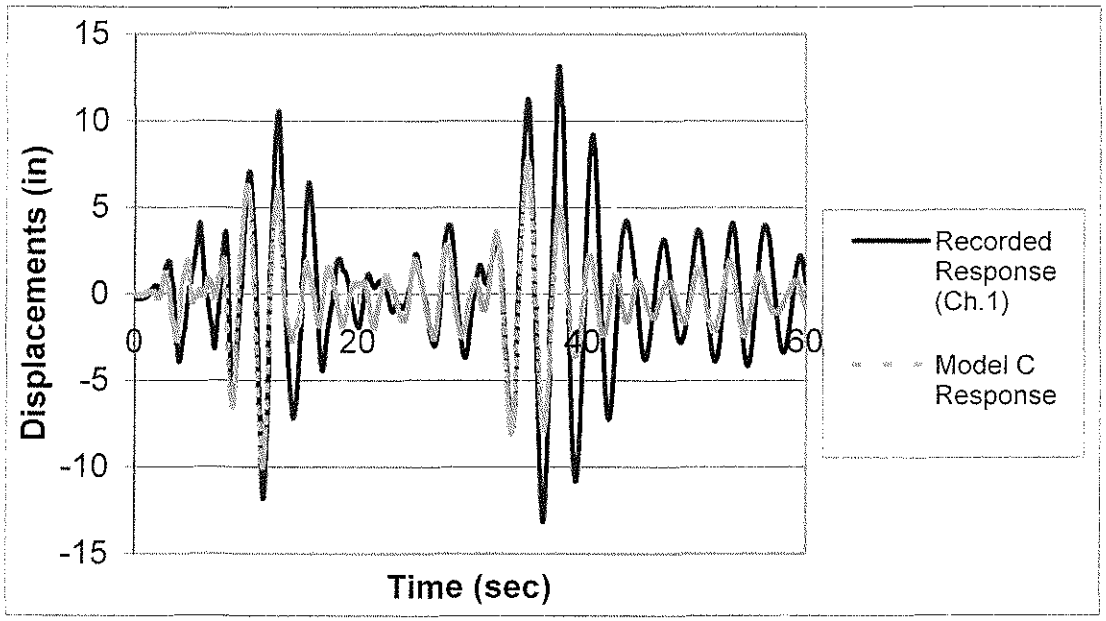

Figure 3-24. Displacement History for Model C

3.6. Model Selection

This section discusses the results obtained for each model to select the model that better represents the recorded response of the structure. Table 3-1 and Table 3-2 show the comparison of the periods and maximum displacements obtained from the displacement responses of the models and the recorded data.

The period of motion for the building at the roof is estimated for six time ranges and the values are shown in Table 3-1. To calculate the period was necessary to count the number of cycles for 10 seconds and divided that number by the number of seconds then calculate the inverse of that number and that was the period for each time range.

Table 3-2 shows a comparison of the drift at the ground, second floor, eight floor and roof for the three models at the time of maximum response. These drifts are compared with the drifts in the recorded motion. A ratio of difference between the modeled and the recorded response is provided as:

$$\text{Ratio of Difference} = \frac{\text{Modeled Drift Value}}{\text{Recorded Drift Value}} \tag{3.6}$$

Table 3-1. Comparison of Frequency values for Models and Record

Model	T(sec) 1–10 sec Roof	T(sec) 11–20 sec Roof	T(sec) 21–30 sec Roof	T(sec) 31–40 sec Roof	T(sec) 41–50 sec Roof	T(sec) 51–60 sec Roof
A	1.48	2.5	2.5	2.5	2.5	2.86
B	2.11	2.5	2.5	2.5	2.5	2.86
C	**2.11**	**2.5**	**2.67**	**3.33**	**2.5**	**2.86**
Rec.	2.67	2.86	3.03	3.33	3.33	2.86

Table 3-2. Comparison of Maximum Deformed Shapes Values

Model / Floor	A (t=11.36 sec)			B (t=11.36 sec)			C (t=11.40 sec)		
	Model	Rec	Ratio Diff	Model	Rec	Ratio Diff	Model	Rec.	Ratio Diff
Ground	0	0.3	NA	0.03	0.3	0.10	**0.48**	**0.2**	**2.4**
Second	1.4	2.7	0.53	1.8	2.7	0.67	**2.4**	**2.6**	**0.92**
Eighth	7.5	8.0	0.94	7.8	8.0	0.98	**8.2**	**8.2**	**1.0**
Roof	10.1	11.2	0.90	9.9	11.2	0.88	**10.0**	**11.6**	**0.86**

The analysis of the data shows that the behavior of Model C better represents the overall recorded response of the structure. The period values of Model C for all the ranges of time analyzed are closer to the values from the recorded response. The deformed shape of Model C closely follows the recorded deformed shape of the structure. In Chapter 4, Model C will be modified by a strength-based relationship to analyze the change in the structural response. Figure 3-25 shows the comparison of

the deformed shape for all the analyzed models and the recorded response at the correspondent time. The biggest improvement between the response of Model B and Model C is in the lower levels (ground and second floor). This is because Model B does not account for the amplified response possibly caused by soil structure interaction. Model B only models the sublevels with a large wall stiffness and this does not allow the model to respond similar to the target structure.

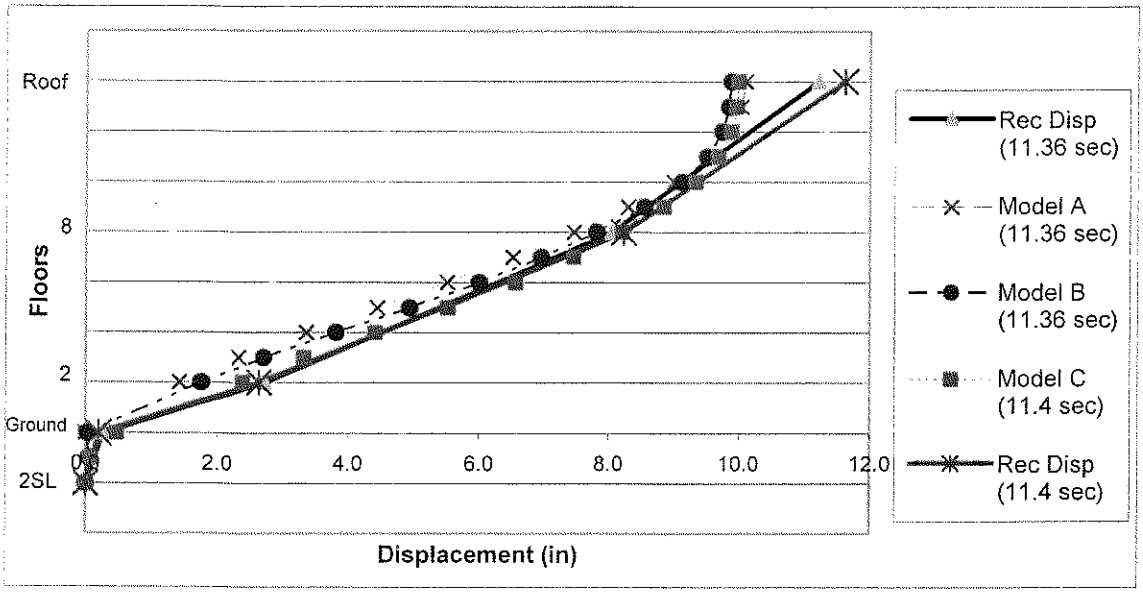

Figure 3-25. Comparison of Modeled and Recorded Deformed Shapes

Figure 3-26 shows a comparison of the displacement history for all models at the roof. Models A and B have almost the same behavior in amplitude and periodicity, while Model C follows most of the behavior for the other two models with a slightly different behavior in few points. At the roof, the behavior of all models appears nearly the same.

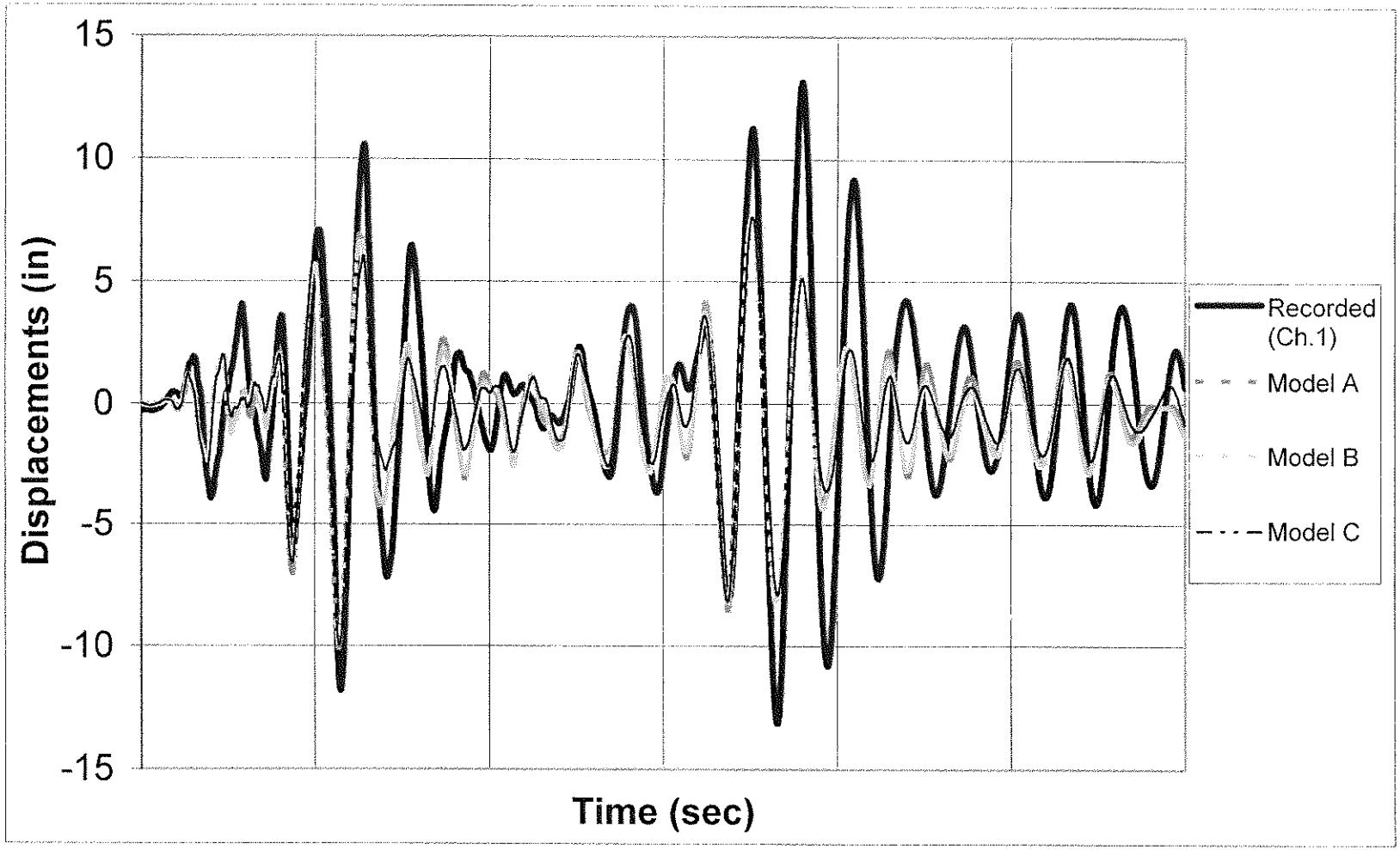

Figure 3-26. Comparison of Displacement History for all Models and Record at Roof (Ch. 1)

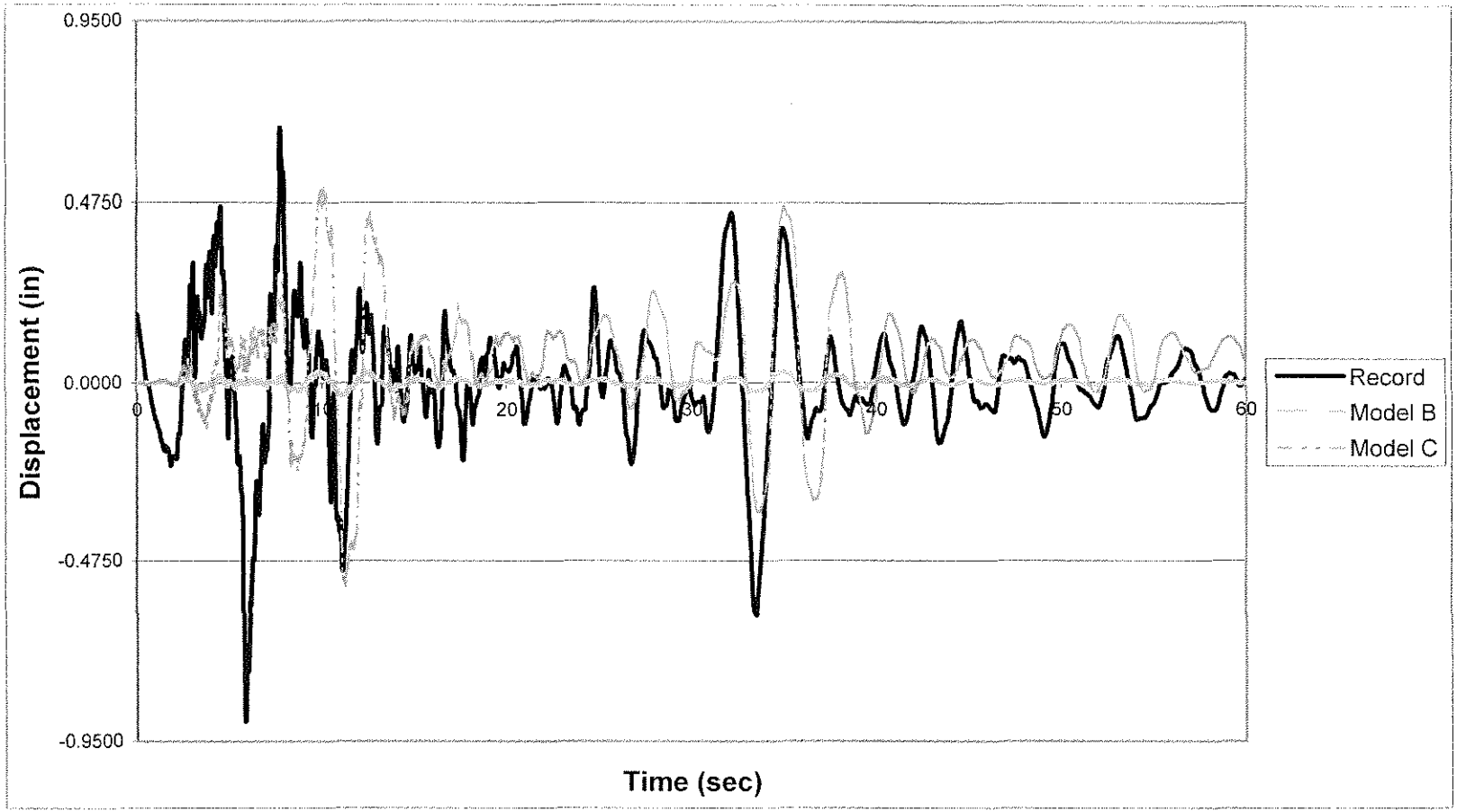

Figure 3-27. Comparison of Displacement History for all Models and Record at Ground Level (Ch. 10)

The most important improvement in the modeling of the target structure is shown in Figure 3-27. The response of Model B at the ground level is shown in the figure with nearly zero displacement value for the entire range of response. Model A is not included because its displacement at the ground level was zero. Model C is able simulate some displacement at the ground level, although the periodicity of response is not similar to the recorded motion for the first 10 seconds of response. After this time, the periodicity is closer in comparison. Fig. 3-27 demonstrates the primary advantage for using Model C to represent the structure in that it better represents the response of the lower levels of the building.

4. Strength-Based Relationship to Modify the Response of the Target Structure

After analyzing all the studied models (Chapter 3), Model C was selected to represent the response of the structure. The similarity of the deformed shape for the model and the actual structure suggest that the reproduced stiffness distribution is similar to that of the actual structure (Figure 3-23, Table 3-1 and Table 3-2). Model B also was evaluated in this chapter and results were compared with the results for the Model C analysis.

Model C was analyzed using a non-linear static analysis routine (LARZ) to estimate the yielded shape of the structure. The strength of the girders for Models B and C were modified with the relationship developed by Kuntz (2001) and analyzed to evaluate the change in the structural response. The modifications and results are discussed in this chapter.

4.1. Description of the Strength-Based Relationship

The objective of the strength-based relationship (Kuntz, 2001) was to improve the structural response of a building system. The manner to improve the response was to encourage the formation of a structural mechanism instead of an intermediate story mechanism (Figure 4-1). By encouraging a structural mechanism to form, yielding in the columns above the base is eliminated and the deformed shape is improved. The structural mechanism is achieved by forcing the yielding to occur in the girders

instead of the columns, as a result an approximate linear distribution of drift will be developed over the height of the structure.

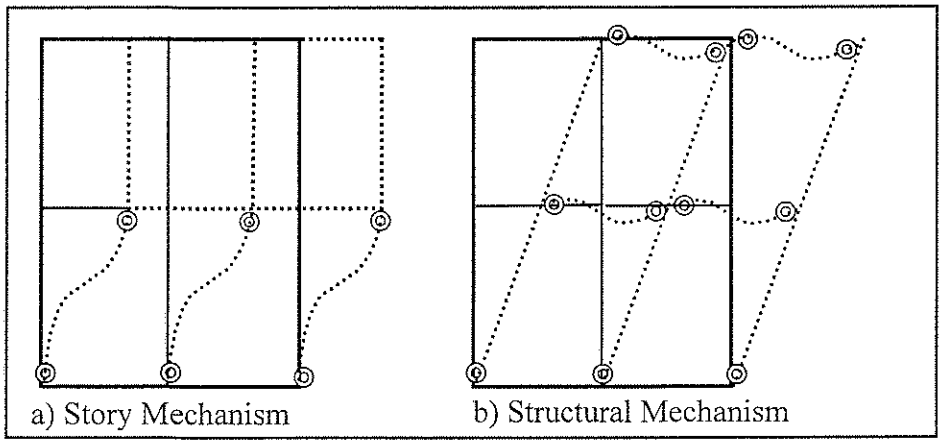

Figure 4-1. Yielding Mechanisms

The strength-based relationship reduces the strength of the girders by a factor that depends on several variables. There is a lower bound to the reduction based on the minimum strength necessary to resist the gravity loads supported by the girders. The equation developed by Kuntz (2001) is presented below:

$$R = 1 + \frac{N_s \cdot N_b \cdot \sqrt{\rho \cdot h}}{7 \cdot (N_b + 1) \cdot \beta \cdot \alpha^2} \qquad (4.1)$$

where: N_s = number of stories

N_b = number of bays

ρ = column reinforcement ratio

h = Column width (inches)

β = Ratio of number of floor levels with reduced girder strength to total number of stories

α = Ratio of top exterior column strength to girder strength

The reduction factor obtained for the target structure was extreme (6.41) as shown in Table 4-1. It was not possible to apply it to the model based on the limitations due to gravity loads and suggested limitations proposed by Kuntz. The values for all the variables used to calculate the strength reduction factor are shown in Table 4-1.

Table 4-1. Factor R Variables Values

Ns	Nb	ρ	h	Mc	# girders	Mg	α	β	R
13	7	0.02	32.9	6105.37	182	7888.52	0.77	0.38	**6.41**

The first variable, Ns, is based in the number of stories above ground, and the target structure has 13 floors above ground. The rho (ρ) value was calculated as an average of the reinforcement ratio for all of the columns in the building. The column width, h, was calculated as the square root of the cross section, because the reduction factor equation was developed based on square columns. To calculate the ratio α was necessary to know the average moment capacity of the columns in the top floor (13 floor) and the average moment capacity of all of the girders above the ground (2 floor to roof). The ratio β was calculated by dividing the number of floor with reduced strength by the total number of floors above the ground. The equation to calculate R is shown above (Eq. 4.1).

Kuntz stated that a reduction factor, R, bigger than 4 was not recommendable to use. This statement is based on practical use and safety issues. The maximum reduction factor allowed based on gravity loads is discussed in section 4.3.1.

4.2. Original Yielding Profile – Static Vs. Dynamic

The yielding profile for models B and C from the dynamic analyses was obtained and compared with the yielding profile from the static analysis. The static analysis results were obtained at a maximum roof drift equal to that obtained in the dynamic analysis. For both models, the profile is nearly the same for the dynamic and static analyses (Figure 4-2 and Figure 4-3).

The static analyses were performed using the latest LARZ version developed by Coll and Lopez at the University of Puerto Rico. The load distribution for the static analysis was based on the FEMA provisions (FEMA 356, 2000). This load distribution was chosen in lieu of the linear distribution based on the recommendations provided by Marsh (2001). The study showed that the load distribution obtained by FEMA provisions produced the largest drift for tall structures with a tall first story. In addition the lower levels tended to deform similar to the first mode shape.

The dynamic analyses were performed using the acceleration records for the target structure subjected to the Northridge earthquake. The maximum roof drift obtained for the dynamic analyses (shown in Chapter 3) was the limiting displacement for the static analyses of Models B and C.

4.2.1. Results - Static vs. Dynamic

The following figures show the obtained results for the static and dynamic analyses of Models B and C. The models analyzed here have girder moment capacities as described in the building plans

The results will be shown for the exterior frames of both models and compared with the results for the interior frames of both models.

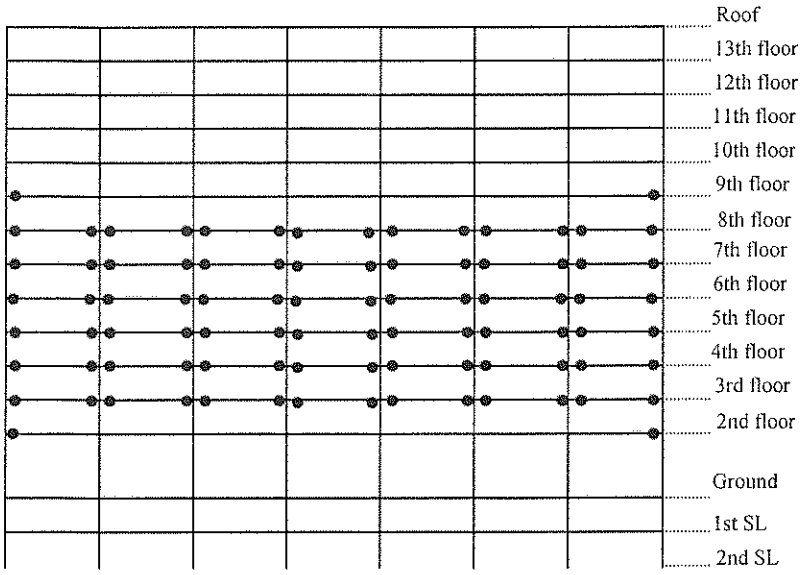

Figure 4-2. Yielding Profile for the Static Analysis / Model B - Exterior Frame

Figure 4-2 and Figure 4-3 show the yielding member in the exterior frame of Model B for the static and dynamic analyses, respectively. Except for the yielding at the 9^{th} level they are identical. The roof drift for the static analysis was 10 inches and for the dynamic analysis was 9.9 inches. The deformed shape at this roof drift for the static model is shown in Figure 4-4 (for the model which includes both the interior and exterior frames) and for the dynamic model was shown in Chapter 3 (Figure 3-15).

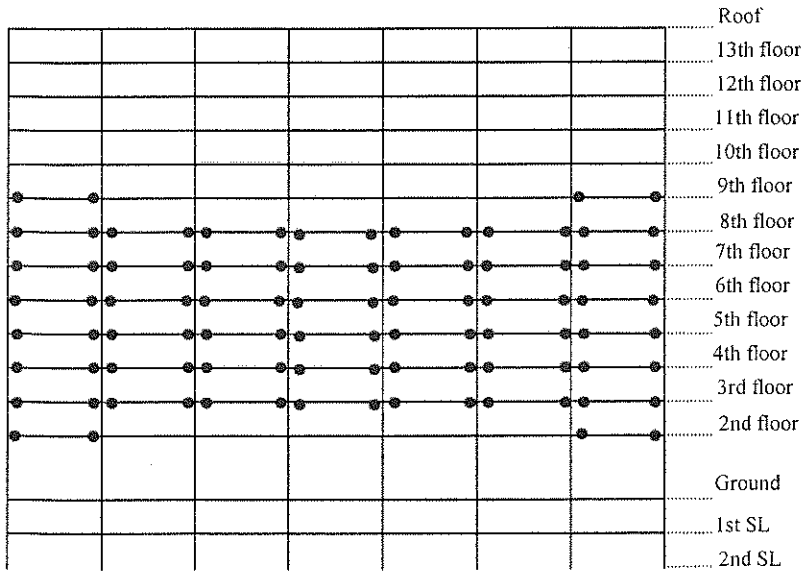

Figure 4-3. Yielding Profile for the Dynamic Analysis / Model B – Exterior Frame

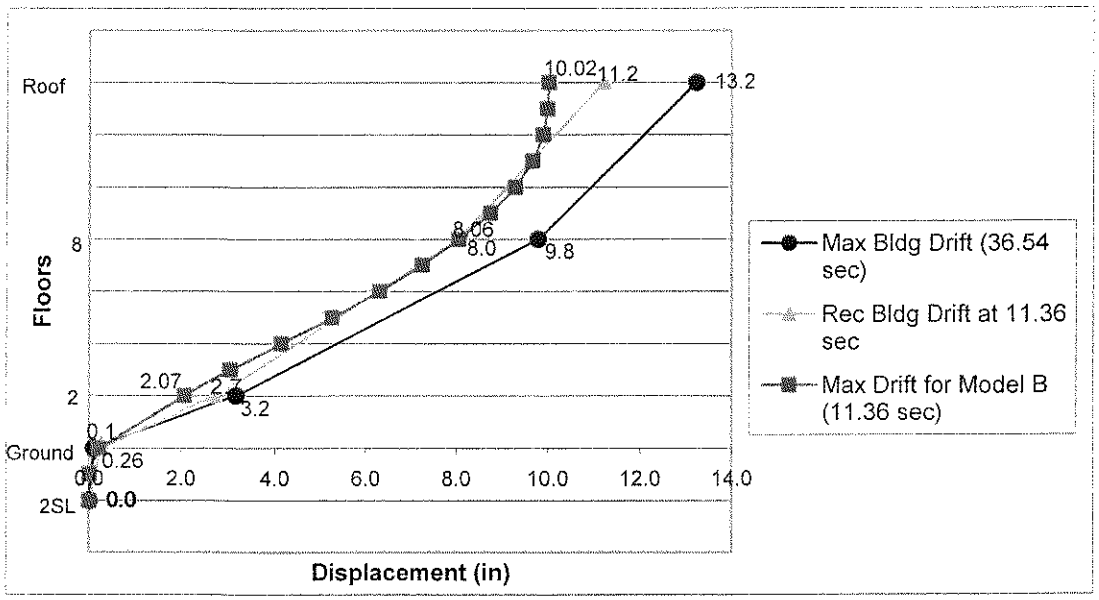

Figure 4-4. Deformed Shape for Model B - Static Analysis

Figure 4-5 and Figure 4-6 show the yielding profile for the interior frame of Model B for the static and dynamic analyses. Both analyses for this frame have the same yielding elements.

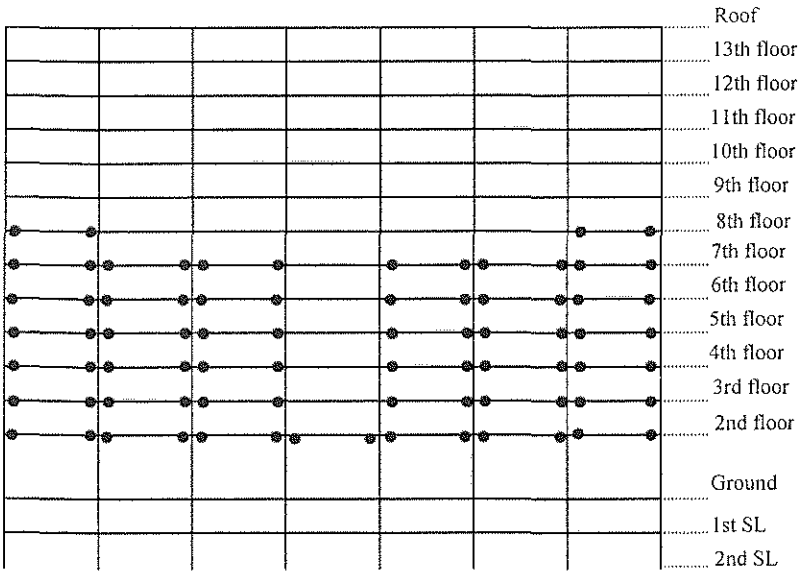

Figure 4-5. Yielding Profile for Static Analysis - Model B / Interior Frame

The similarity between the static and dynamic results for the interior frame demonstrates that the lateral force profile selected was appropiate. The base shear values for the static and dynamic analyses of Model B were 2174 kips and 2721 kips respectively. That fact that the dynamic analysis has a larger base shear value is confirmed by the results because the dynamic analysis produced more yielded elements than the static analysis.

Figure 4-7to Figure 4-10show the results for the static and dynamic analyses of Model C. It can be observed that for this model the results for both analyses are nearly identical.

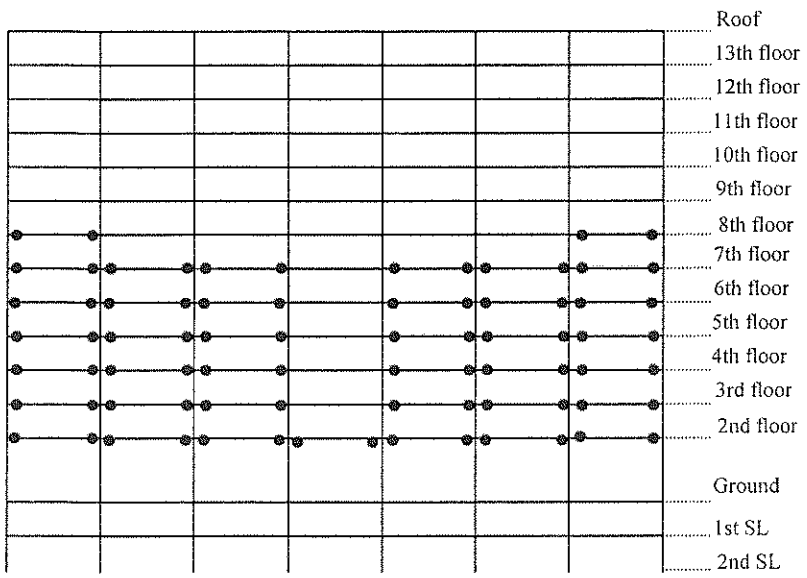

Figure 4-6. Yielding Profile for the Dynamic Analysis - Model B / Interior Frame

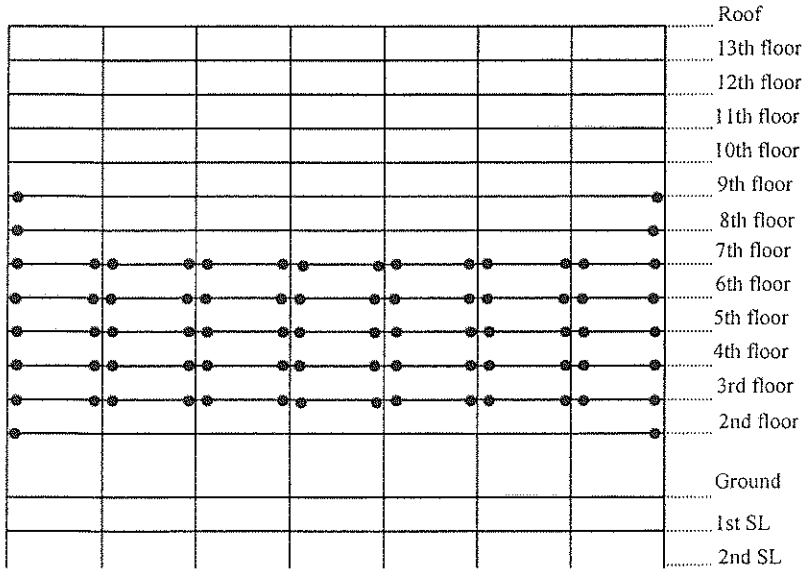

Figure 4-7. Yielding Profile for Static Analysis - Model C / Exterior Frame

The yielding profile for Model C resemble the results obtained for Model B. The major difference is in the 8^{th} floor. The dynamic analysis for Model B shows all the girders for the 8^{th} floor yielded whereas the dynamic analysis for Model C only

shows the connection between the exterior columns and girders yielded. The maximum base shear force reached by the dynamic analysis of Model B was 2721 kips while the base shear force for the dynamic analysis of Model C was only 2457 kips. The smaller stiffness value for the walls in the sublevels will be the reason for the change on the base shear force value and consequently in the yielding behavior of the structure.

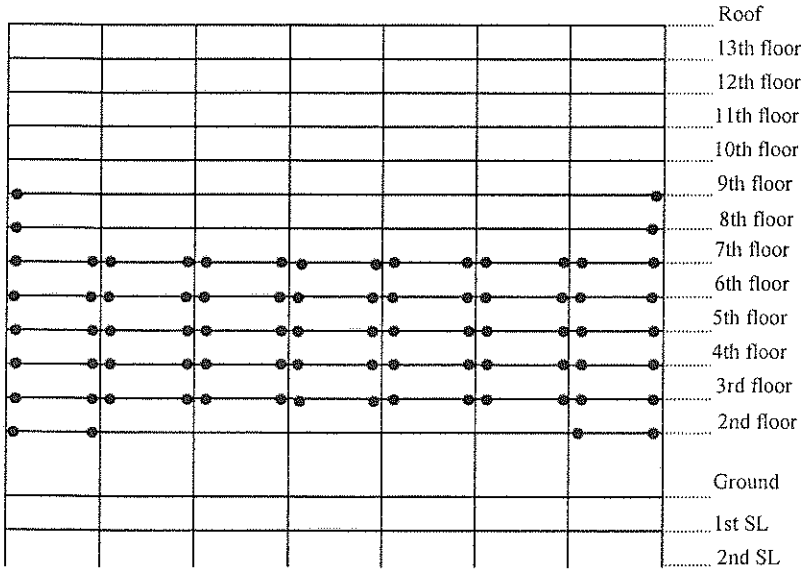

Figure 4-8. Yielding Profile for Dynamic Analysis - Model C / Exterior Frame

The difference between the static and dynamic profiles for Model C is located on the interior frame on the 7^{th} and 8^{th} floors. With the reduced stiffness of the frame, the base shear force necessary to cause yielding was reduced as well. The base shear force reached by the dynamic analysis of Model C was 2457 kips while the base shear force for the static analysis was 2130 kips.

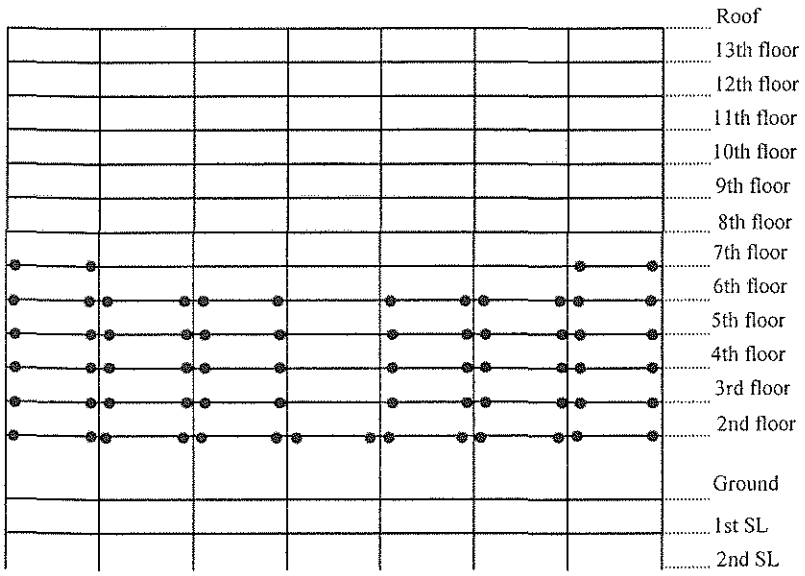

Figure 4-9. Yielding Profile for Static Analysis - Model C / Interior Frame

The fact that the yielding profile for both analyses of Model B and the dynamic analysis of Model C are exactly the same for the interior frame demonstrates that there is a range of values of base shear force necessary to produce that specific yielding profile. This also reflects the fact that yielding between the two frames will vary based on the type of force (either static or dynamic) and the stiffness properties of the frames. The base shear force reached by the dynamic analysis of Model C is approximately 2457 kip, which is between the values reached by the analyses of Model B, 2174 kips for the static and 2721 kips for the dynamic. As stated before, the static analysis of Model C reached the smallest base shear value of 2130 kips. This value was less than the minimum base shear force necessary to produce the same yielding profile for the interior frame as obtained in the dynamic analysis of Model C and both analyses for Model B.

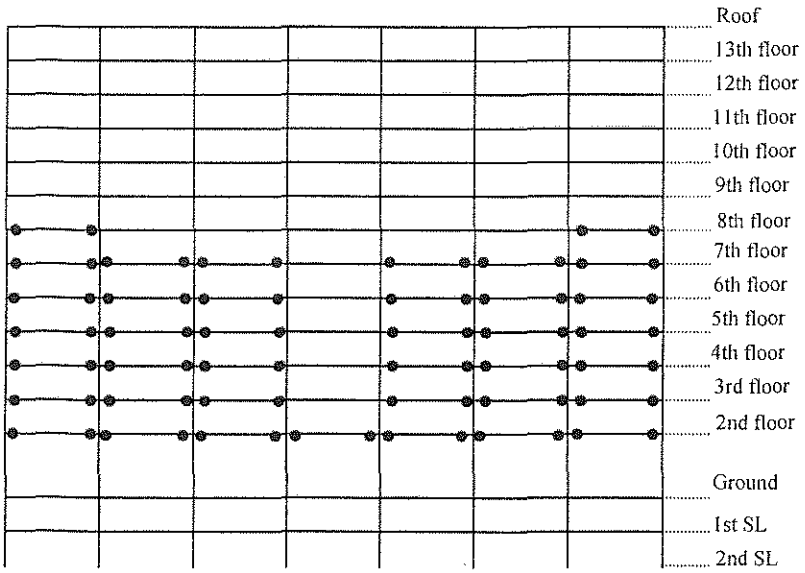

Figure 4-10. Yielding Profile for Dynamic Analysis - Model C / Interior Frame

The results shown in this section will be a point of reference to analyze the results of the modified models. The results for the modified models will be shown and discussed in the following section.

4.3. Application of Factor R to Target Building –Models B and C

4.3.1. Strength Check

The value of the reduction factor, R, is limited by the minimum value of strength required to resist gravity loads for the girders. The load used to check the minimum strength values in the girders was based on the requirements of ASCE 7-98 (ASCE, Table 4.1, 2000). The ASCE 7-98 code requires that lobbies and first floor corridors in office buildings have a design live load of 4.79 kN/m^2 (100 psf), offices a design live load of 2.40 kN/m^2 (50 psf), and corridors above the first floor should have a live load of 3.83 kN/m^2 (80 psf). An approximate minimum value for live

loads was taken as 2.40 kN/m^2 (50 psf) and was used to check the gravity load demands in the modified girders.

Using Equation 9.1 of the ACI building code (1999), the ultimate load (w_u) was calculated:

$$w_u = 1.4DL + 1.7LL \tag{4.2}$$

where: DL = Total Dead Load

LL = Live Load

Approximate design moments were calculated using the moment coefficients as given in Section 8.3.3 of the A.C.I. building code (1999). The maximum negative (M_{max-}) and positive (M_{max+}) design moments were calculated as follows:

$$M_{max-} = -\frac{w_u l_n^{\,2}}{10} \tag{4.3}$$

$$M_{max+} = \frac{w_u l_n^{\,2}}{14} \tag{4.4}$$

where:

l_n = clear span length for positive moment and average clear spans for negative moment.

Using formulas (4.3) and (4.4) the ultimate moments for the girders were calculated to know how much reduction of the moment capacity was possible. The location of all the girders for which the strength was modified by factor R is shown in Figure 4-11 and Figure 4-12. In Table 4-2 are shown the demand moments and the moment values resisted by the modified girders in both frames. As can be seen in Table 4-2 the moment values for most of the other girders were reduced by a common

factor value. On the other hand, the middle girders from 9^{th} to 13^{th} floors for the interior frame were modified by a different factor, this was because those girders have a smaller capacity moment. After analyzing these data it become apparent that the moment capacity for girder 1 and girder 2 (Figure 4-11) could not be reduced because the original strength value was smaller than the maximum negative moment demand. The actual moment values were divided by 1.5, therefore the modified girders strength were approximately 66% of their original strength values. In Table 4-2 girder 5 has two values of original and reduced moment capacity because the capacities vary and only the maximum and minimum values are reported. The maximum reduction factor for each girder type was not possible to use because it caused the model to be instable, possible yielding occur at the same time in different areas of the building and that caused excessive displacement and instability of the model.

The modified model included all the members reduced by its correspondent factor. The results of the different models allow comparing the results for a model with a stiff foundation (Model B) and a model with a softer foundation (Model C). In addition to the reduction factor modification analysis, the models are analyzed for different earthquake demands. The acceleration records will demonstrate the influence of earthquake frequency content and intensity on the response of the models. In the following section (4.3.2) the results for both models will be discussed.

Table 4-2. Maximum Moment Reduction by Gravity Loads

Moment check:	DEMAND		CAPACITY	
Girder	Mu_{neg} (kip-in)	Mu_{pos} (kip-in)	My_{orig} (kip-in)	$My_{reduced}$ (kip-in)
1	-4905.8	3504.1	4228	4228
2	-5108.0	3648.6	4228	4228
3	-4505.3	3218.1	5860	3856
4	-4691.1	3350.8	5860	3856
5	-4707.6	3362.5	6788 - 8335	4466 - 5483
6	-4323.3	3088.1	7890	4002
7	-4323.3	3088.1	6792	4468
8	-4323.3	3088.1	4852	4323

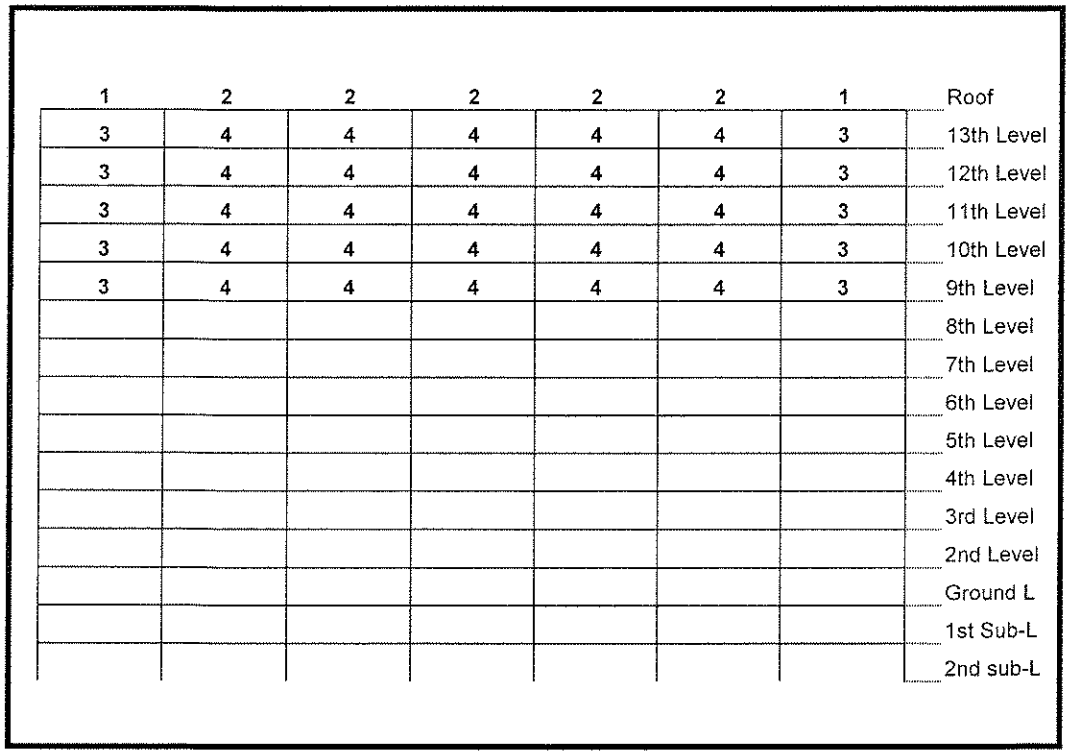

Figure 4-11. Exterior Frame - Modified Girder Locations

5	5	5	5	5	5	5	Roof
6	6	6	8	6	6	6	13th Level
6	6	6	8	6	6	6	12th Level
6	6	6	8	6	6	6	11th Level
7	7	7	8	7	7	7	10th Level
7	7	7	8	7	7	7	9th Level
							8th Level
							7th Level
							6th Level
							5th Level
							4th Level
							3rd Level
							2nd Level
							Ground L
							1st Sub-L
							2nd sub-L

Figure 4-12. Interior Frame - Modified Girder Locations

4.3.2. Results

The modified (using factor R) and unmodified models B and C are compared and analyzed using three earthquake accelerations. The additional accelerations were chosen to be greater than the original recorded input from the structure. From the results obtained in section 4.2.1, it was evident that the demand over the structure was not sufficient to create a yielding mechanism. In order to evaluate the improvement in the response of the target structure by the application of factor R, it is desired to have an initial yielding mechanism in the structure.

Three sets of results were analyzed and compared for the modified and unmodified models. The compared sets of results were: yielding location, deformed shapes, and story drift ratio.

4.3.2.1. Acceleration Inputs

The three earthquakes chosen were:

1. San Fernando – Pacoima Dam record (1971)
2. Kobe (1995)
3. Northridge – Original Building record

The first record has a high demand (1.2 g, peak ground acceleration) and high frequency content as shown in Figure 4-13. The record was measured on the S-E direction. This record was chosen because it will induce a great demand on the target structure. In addition, the source of this earthquake could eventually affect the target structure.

The second record has lower dominant frequencies but still has a large intensity. The peak ground acceleration was 0.81 g, its epicentral distance is 1 Km (1.6 miles) and is a NS component. This record was used to analyze the influence of low frequencies in the target structure. The acceleration record for this earthquake is shown in Figure 4-14.

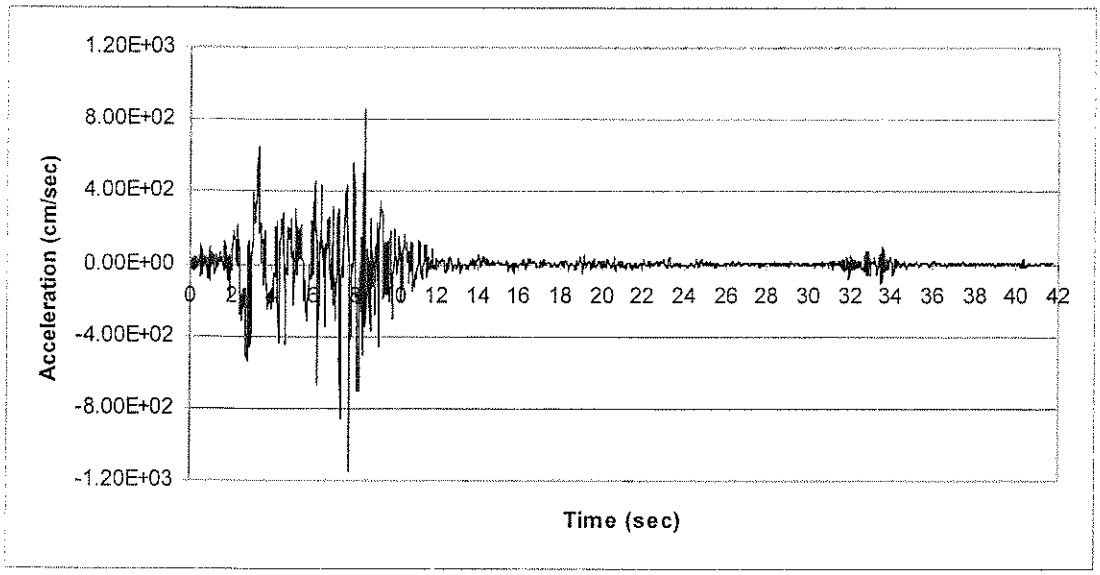

Figure 4-13. Pacoima Dam Acceleration Record

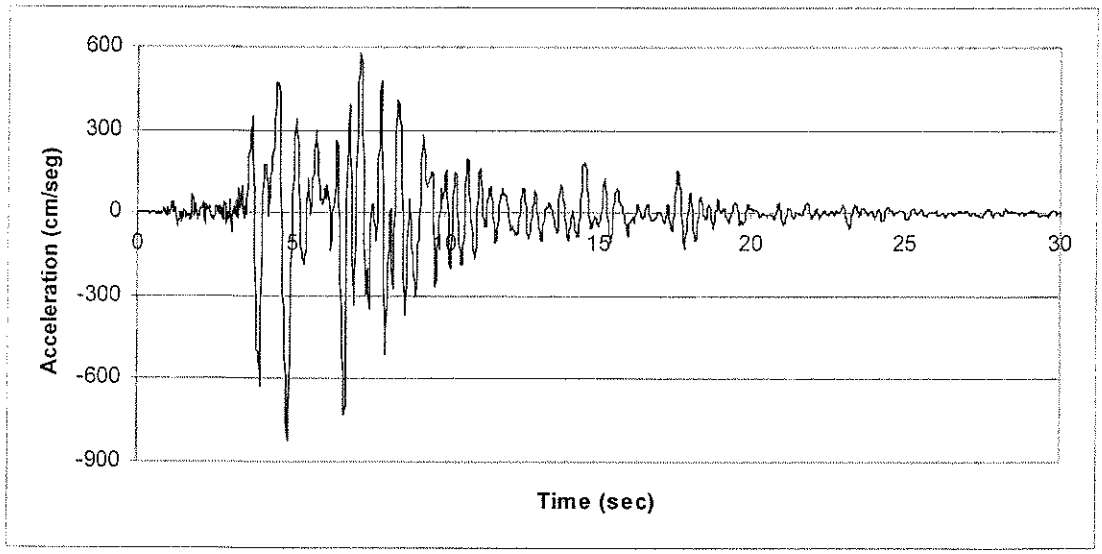

Figure 4-14. Kobe Acceleration Record

The fourth record was the actual recorded accelerations for the target structure. The accelerogram for input channel 13 was shown in Figure 3-22.

4.3.2.2. Yielded Profiles for San Fernando – Pacoima Dam Record

The first set of results discussed is the yielding locations for the exterior and interior frames for the unmodified and modified models.

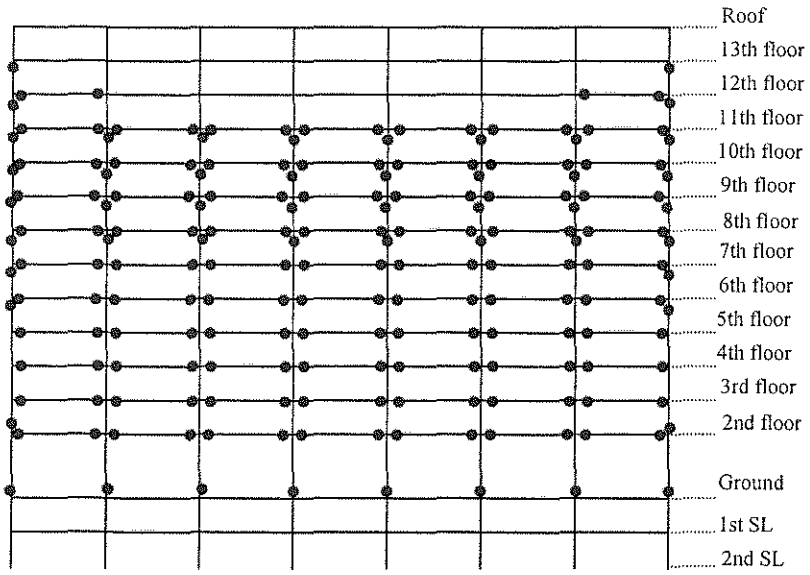

Figure 4-15. Yielding Profile for Unmodified Model B - Exterior Frame

It can be observed in Figure 4-15 that there is a interstory mechanism for this model because all of the columns in the ground floor reached yielding at the bottom and all of the columns in the 7^{th} floor reached yielding at the top. This interstory mechanism agreed with the results found by Marsh (2001) in her comparative study for this type of structure. Between the 7^{th} and 10^{th} floors were found interstory mechanisms where the top of the columns in the lower floor and and the top of the column in the upper floor yielded causing a one story mechanism. Figure 4-16 shows the results for Model B after being modified by Factor R. It is observed that the lower interstory mechanism did shift the upper limit to the eight floor and the upper one-story mechanisms move upward until the 12^{th} floor. for the modified Model B in the

exterior frame, however the one story mechanisms remain in the upper section of the structure.

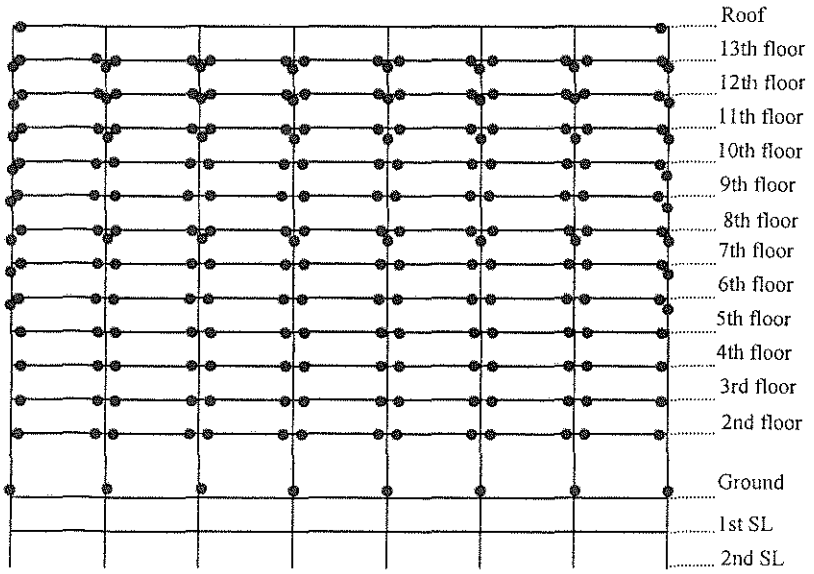

Figure 4-16. Yielding Profile for Modified Model B - Exterior Frame

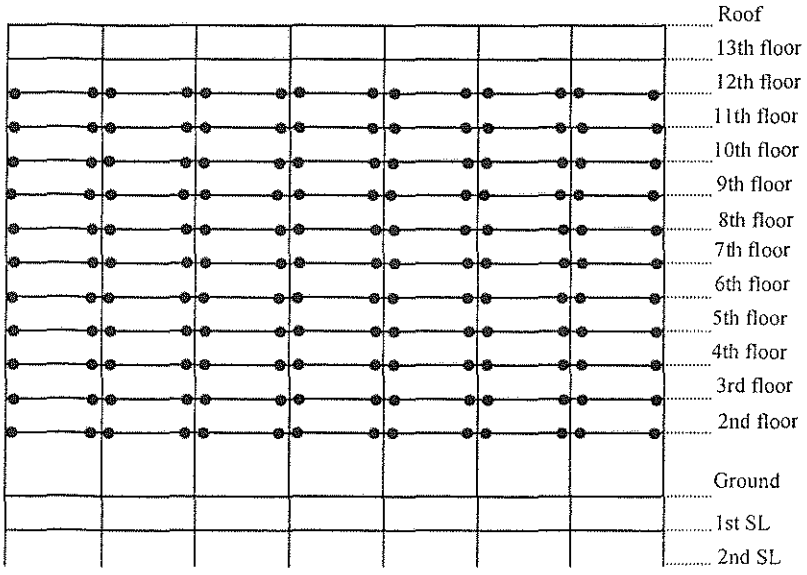

Figure 4-17. Yielding Profile for Unmodified Model B - Interior Frame

As expected, the interior frame for the unmodified model did not develope a yield mechanism. This frame has a greater stiffness value than the exterior frame, consequently it was likely that it would not develop a yield mechanism. It is noted that the modified model response had yielded girders in higher levels than the original model. This is the expected behavior for modified models because it will be the path to follow if a structural mechanism is desired.

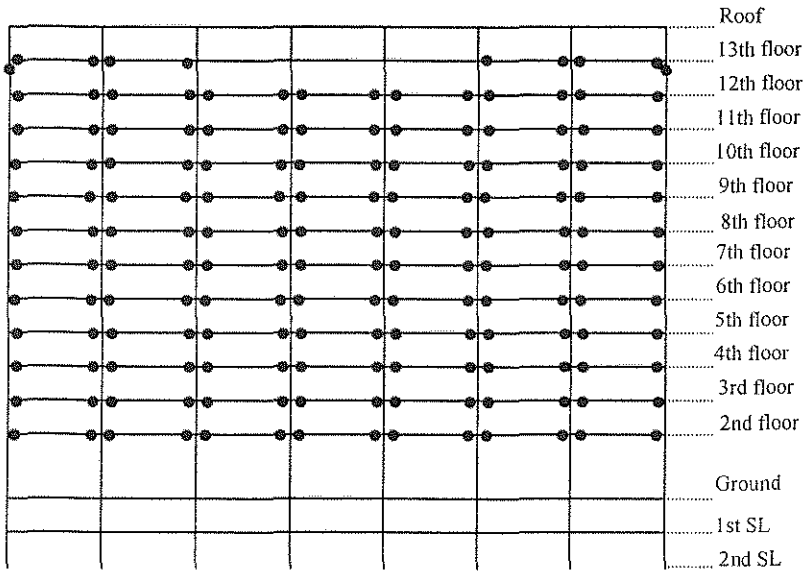

Figure 4-18. Yielding Profile for Modified Model B - Interior Frame

The presented results for Model B showed that is beneficial to apply the strength reduction factor R to structures with stiff foundations because it helps to avoid the formation of interstory yield mechanisms in the lower portion of the structure. It is necessary now to evaluate the results for structures with softer foundations, as represented by Model C.

In this occasion the model did not reached a yielding mechanism, this could be explained on the basis that the softer foundation provides a higher damping ratio and helps the structure to have a better response. Because this model did not developed any yielding mechanism and almost all girders reached yielding, no improvement can be expected from the modified model.

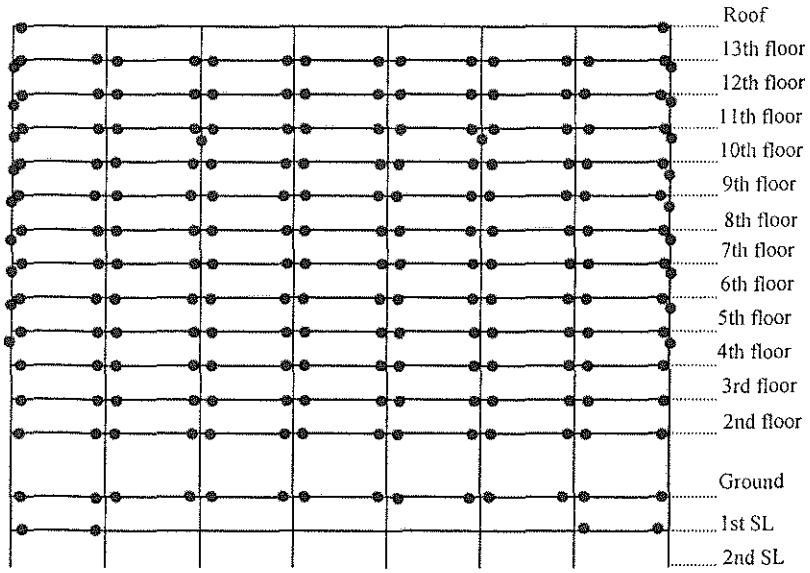

Figure 4-19. Yielding Profile for Unmodified Model C - Exterior Frame

It can be observed on Figure 4-20 that the yielded profile for the modified model is exactly the same as for the unmodified model. There is no improvement or change on the structural behavior of both models. Because the exterior frame is more likely to develop improvements in the response, due to the stiffness values being the smallest of the two frames, is expected that no improvement will be shown for the interior frames. The interior frame has the same yielding pattern for the modified and unmodified models, and are shown in Figure 4-21.

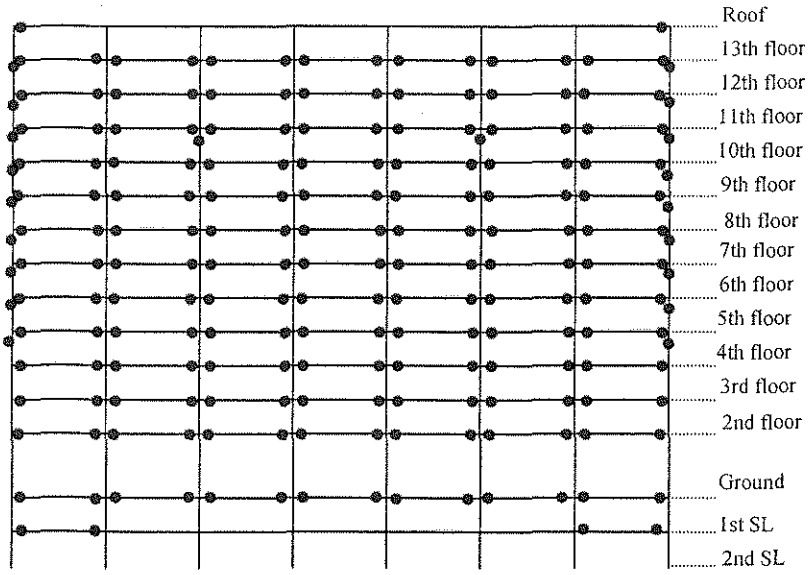

Figure 4-20. Yielding Profile for Modified Model C - Exterior Frame

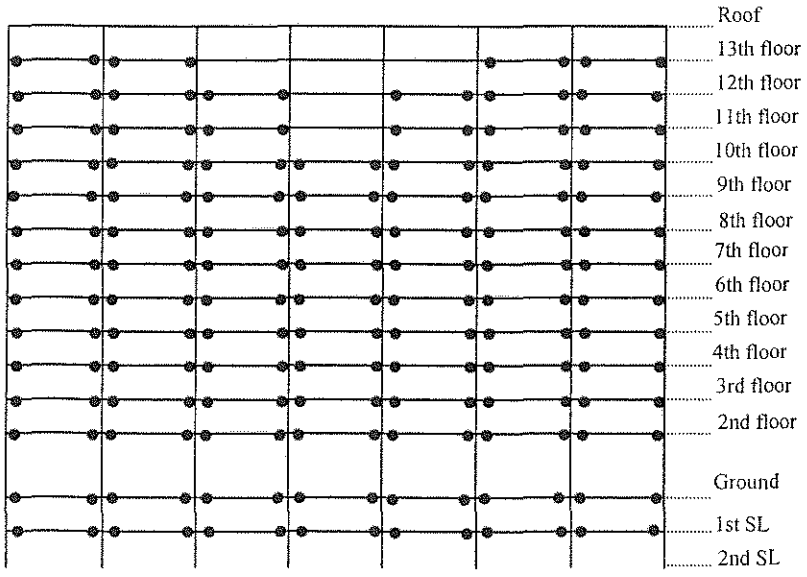

Figure 4-21. Yielding Profile for Unmodified and Modified Model C - Interior Frame

Analyzing these results for the San Fernando earthquake for Models B and C, it is apparent that the strength reduction factor R has a good influence on the response

of structures with stiff foundation, whereas it does not seem to have any influence on the improvement of the response of structures with a soft foundation.

4.3.2.3. Deformed Shapes and SDR for Pacoima Dam Record

Figure 4-22 shows the deformed shapes for all four models, unmodified and modified Models B and C. Looking at the deformed shapes, the change between the response of the unmodified and modified Models B and C seems to be nearly the same. Yet, the deformed shape of the unmodified Model C appears more linear than the response of the unmodified Model B.

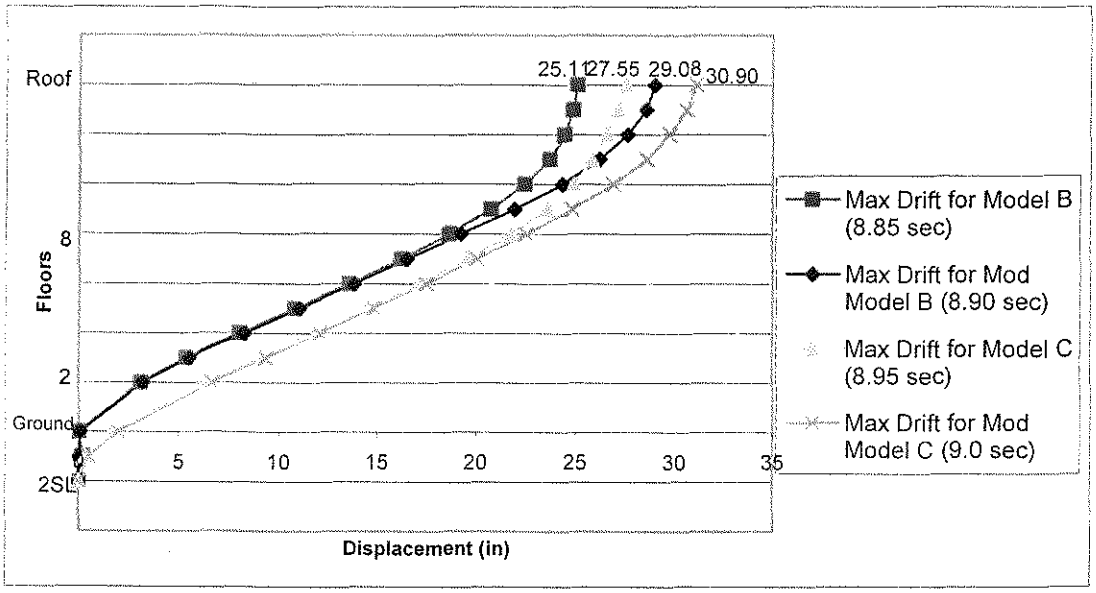

Figure 4-22. Deformed Shapes for all Models Subjected to Pacoima Dam Record

The interstory drift ratios (SDR) are shown for each model in the Figure 4-23 and Figure 4-24. For Model B it is observed that the SDR values for the modified model are more uniform from the 3rd through the 10th floors. It is observed as well that there was a reduction on the SDR values for the two sublevels where there was a wall with a large stiffness value. The top stories showed an increase on the SDR

because the reduction of the strength of the girders induced the structure to have a more uniform SDR by more evenly redistributing the drift over the total height of the structure.

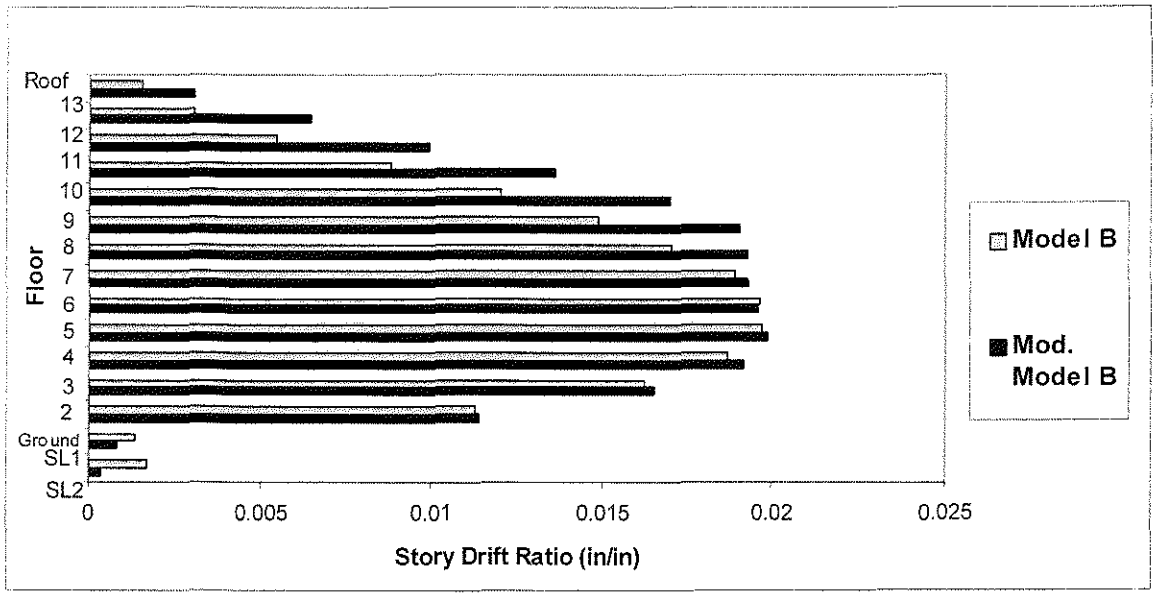

Figure 4-23. Comparison of SDR Values for Unmodified and Modified Model B

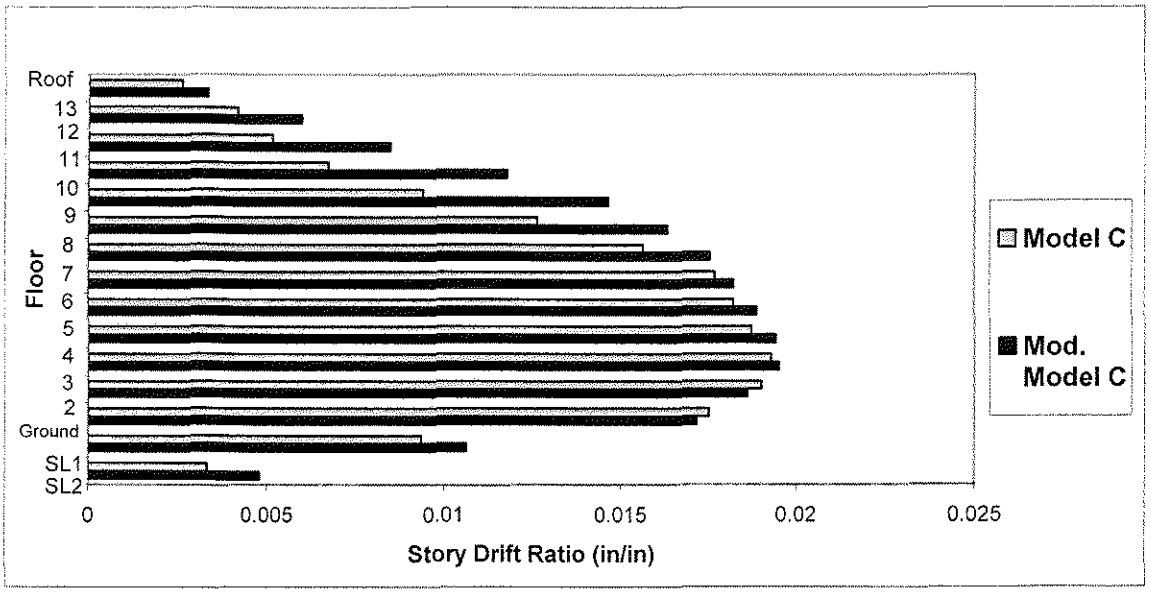

Figure 4-24. Comparison of SDR Values for Unmodified and Modified Model C

Factor R does help the interstory drift response of model C. The SDR increased for all of the floors of the modified Model C, which may be explained because the softer foundation is inducing larger displacements in the structure.

For this specific earthquake the girder strength reduction factor was not able to help the response of the structure substantially because the demand was very high and the structure was not able to resist it.

The base shear value for the unmodified Model B was 10593 kips and for the modified Model B was 10226 kips.

4.3.2.4. Yielded Profiles for Kobe Record

This section will have the same format as section 4.3.2.2. The yielding profile for both models will be shown and analyzed first.

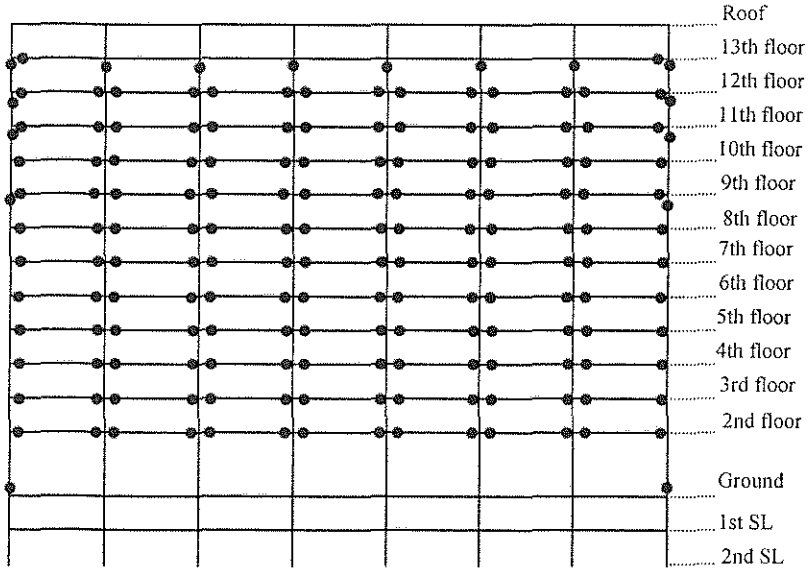

Figure 4-25. Yielding Profile for Unmodified Model B – Exterior Frame

This record affects the structure creating a one story yield mechanism between the 11th and 12th floor of the structure. It produced yielding on the top columns of the 11th and 12th floors and yielded all the girders at the 12th floor. The modified model helped to improve the yield profile of the structure; there is no mechanism present, as it can be observed in Figure 4-26. The columns in the 11th floor did not reached yielding and additional girders on the top floors (13th and roof) yielded to improve the deformed shape of the structure (shown in section 4.1).

For the modified Model B has fewer yielded columns on the 11th floor and redistributes the demands to include almost all of the 13th floor girders.

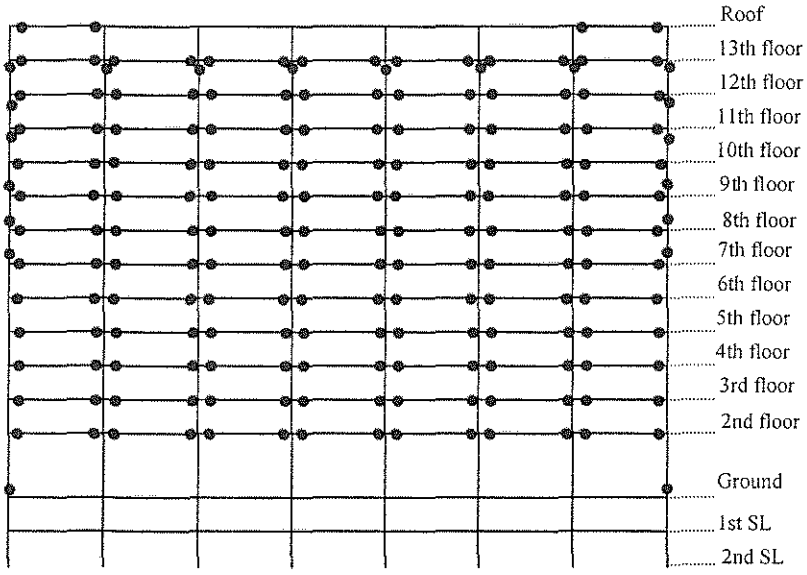

Figure 4-26. Yielding Profile for Modified Model B – Exterior Frame

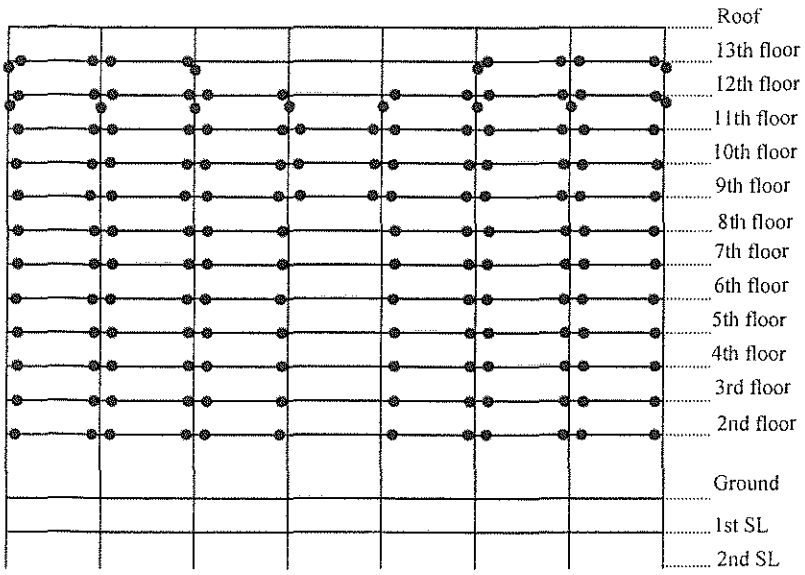

Figure 4-27. Yielding Profile for Unmodified Model B - Interior Frame

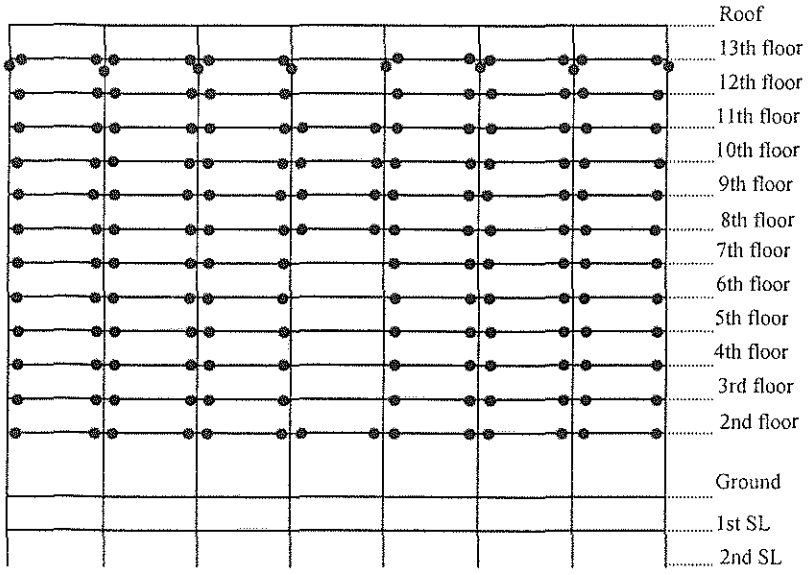

Figure 4-28. Yielding Profile for Modified Model B - Interior Frame

Comparing Figure 4-28 to Figure 4-6 is evident how the structure is being subjected to a much larger demand. In Figure 4-6 the yielded elements are only girders through the 8th floor where as in Figure 4-28 the yielded elements include columns and yielded elements are widespread through the entire structure.

Figure 4-29 and Figure 4-30 show the results for the unmodified and modified Model C for the exterior frame. As before is visible how the srength reduction factor helps to reduce column yielding on the model.

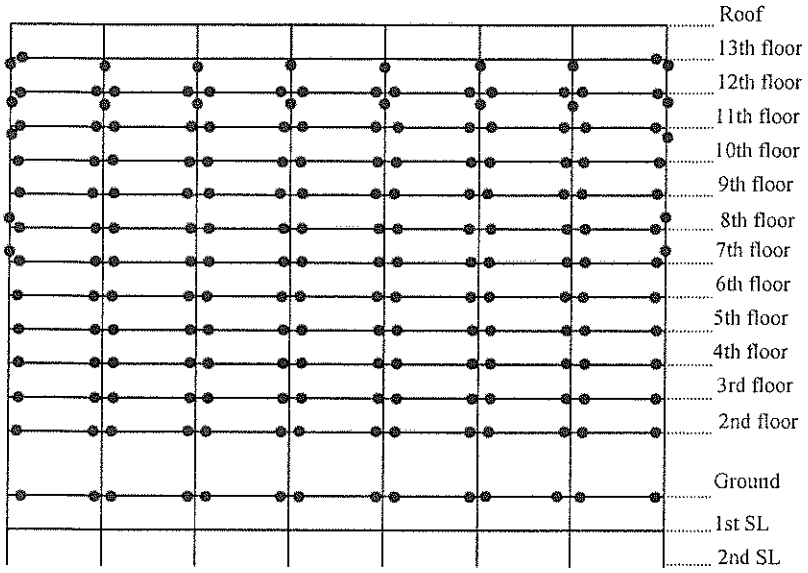

Figure 4-29. Yielding Profile for Unmodified Model C - Exterior Frame

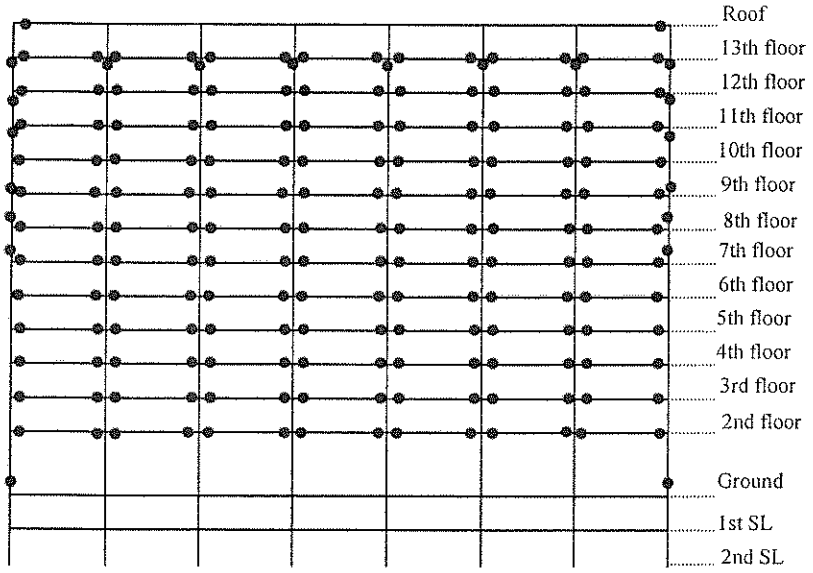

Figure 4-30. Yielding Profile for Modified Model C - Exterior Frame

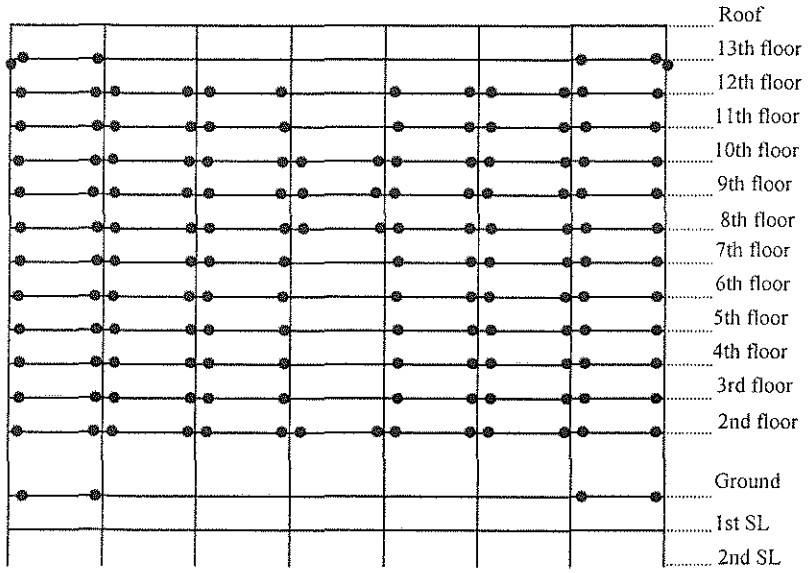

Figure 4-31.Yielding Profile for Unmodified Model C - Interior Frame

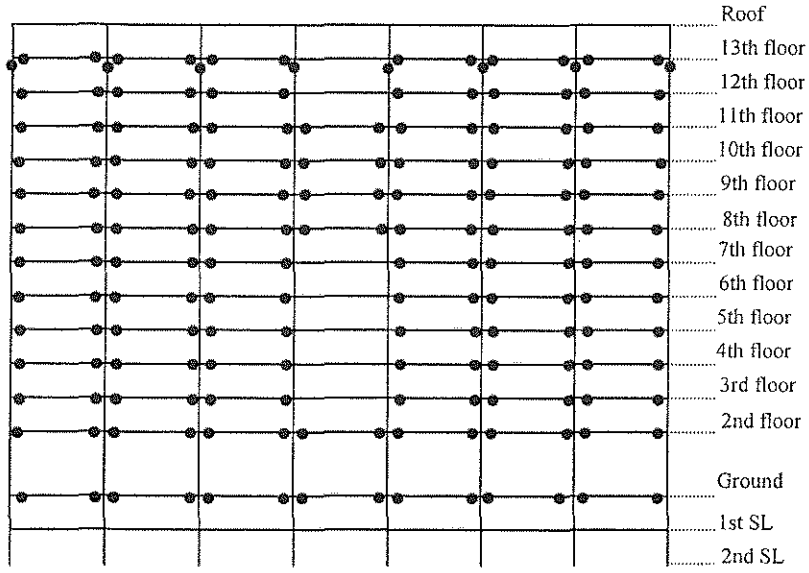

Figure 4-32. Yielding Profile for Modified Model C - Interior Frame

The interior frame yielding profile for the modified model does not seem to show an improvement for the structural behavior (Figure 4-31 and Figure 4-32). In this case more columns in the 11^{th} floor reached yielding. This behavior may be attributable to the response that the specific earthquake has induced in the structure

because this specific earthquake has lower frequencies than the Pacoima Dam record that may cause bigger displacements in a softer model.

4.3.2.5. Deformed Shapes and SDR for Kobe Record

Analyzing the deformed shapes for all models it is apparent that for this acceleration record the strength reduction factor does not help to improve the response (Figure 4-33). None of the models show a linear deformed shape and all of them follow almost the same deformed shape.

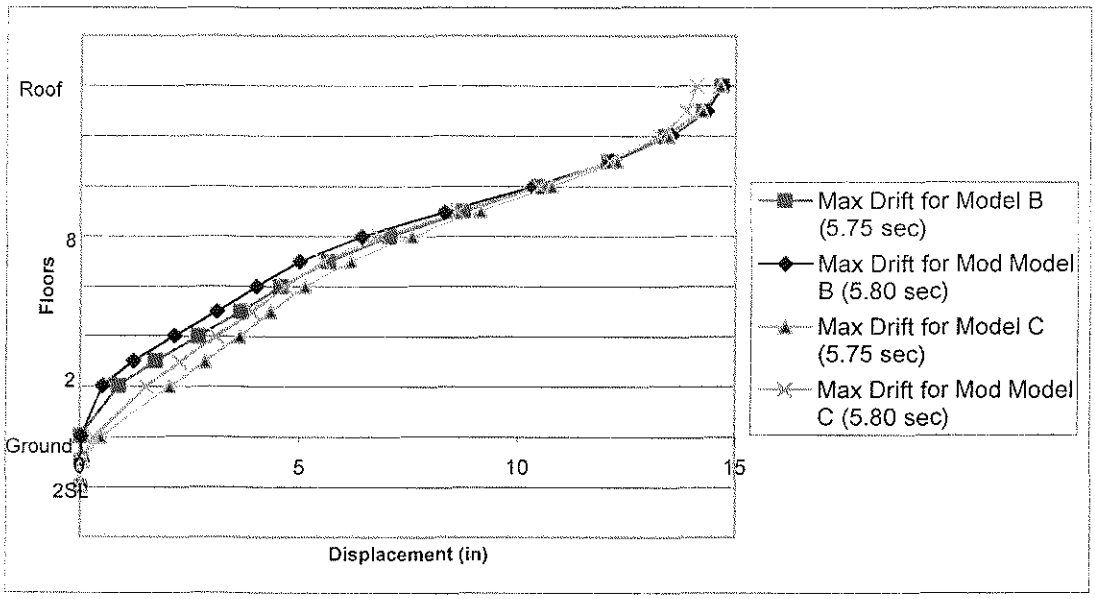

Figure 4-33. Deformed Shapes for all Models Subjected to Kobe Record

This acceleration record seems to excite the structure in such a way that is not possible to improve its behavior substantially, however yielding in columns is reduced. The reason for this response may be the natural frequencies of the building and the frequency of the acceleration record.

The next set of results are the SDR for all models. Figure 4-34 and Figure 4-35 show that the SDR values tend to be different for every floor with the largest

SDR at the top floors. Usually this is not typical, as the lower levels of RC frames are subjected to large SDR demands. It appears that the acceleration record excited a particular response of the structure that induced larger demands in the upper floors.

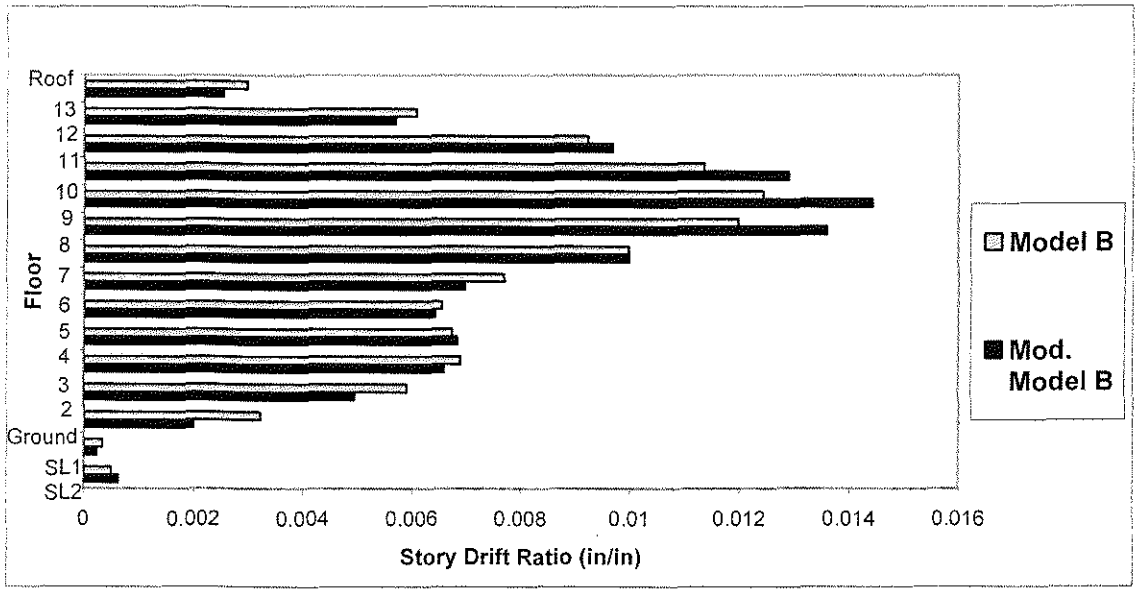

Figure 4-34. Comparison of SDR Values for Unmodified and Modified Model B

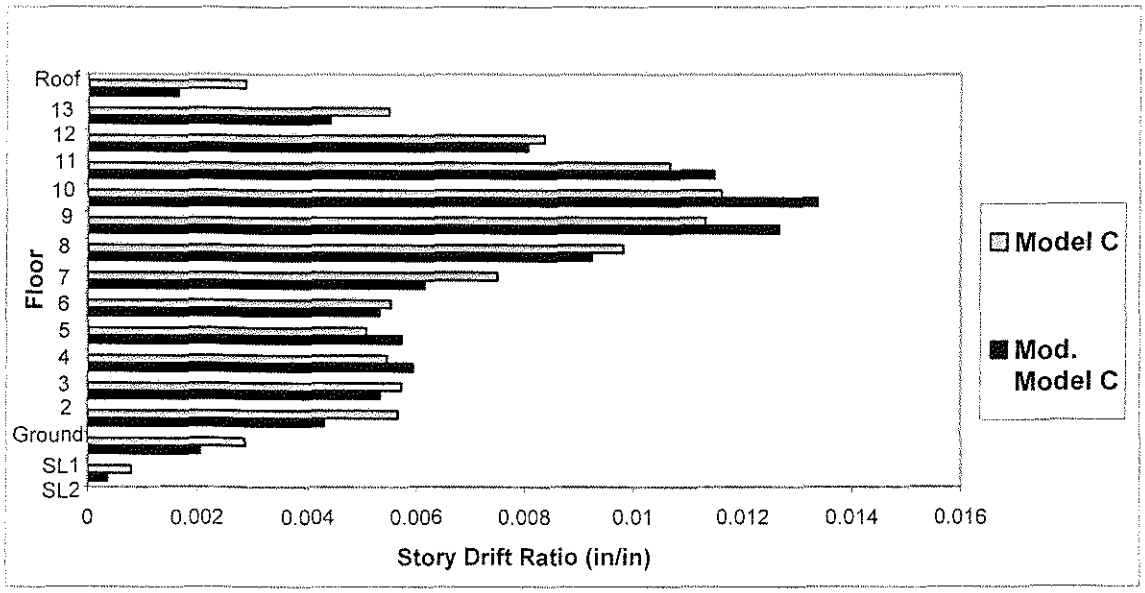

Figure 4-35. Comparison of SDR Values for Unmodified and Modified Model C

4.3.2.6. Yielded Profiles for Northridge – Original Building Record

The yielding profiles for Models B and C for the dynamic analysis were shown in section 4.2.1. Consequently in this section only the yielding profiles of the strength modified models will be shown.

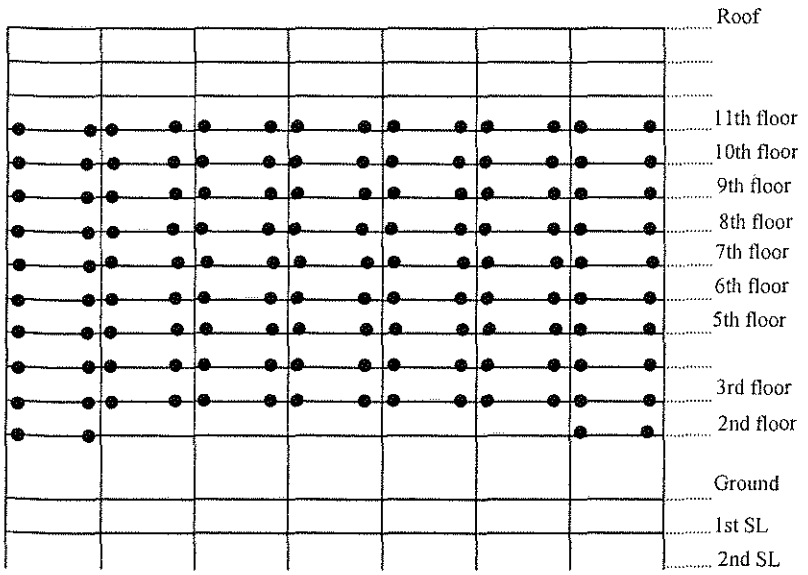

Figure 4-36. Yielding Profile for Modified Model B - Exterior Frame

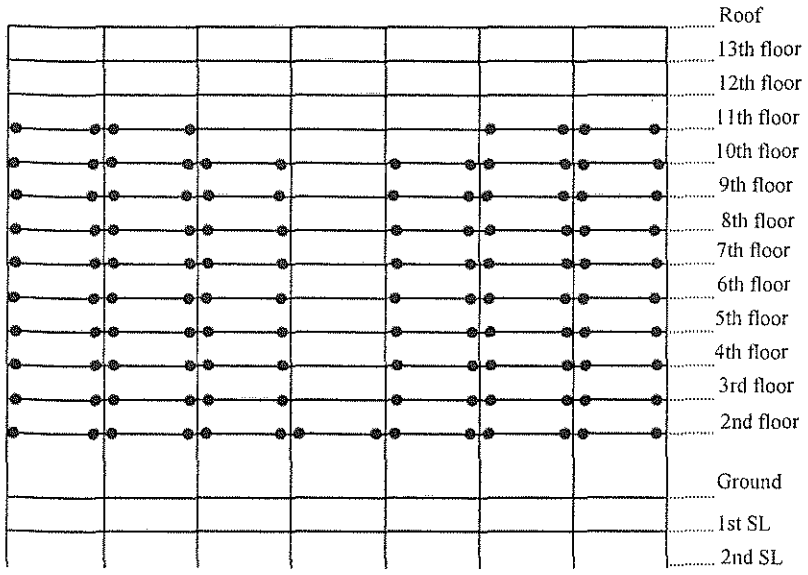

Figure 4-37. Yielding Profile for Modified Model B - Interior Frame

The yielding profiles for the modified Model B subjected to Northridge are shown in Figure 4-36 and Figure 4-37. Comparing Figure 4-3 with Figure 4-36 and Figure 4-6 with Figure 4-37 it is observed that the yielding profile changes between unmodified and modified cases. Before the strength reduction factor was applied to the model the yielded girders for both frames reached different floors, for the exterior frame yielded girders were present only until the 9^{th} floor whereas for the interior frame the yielded girders only reached the 8^{th} floor (Figures 4-3 and 4-6). For the modified model (Figures 4-36 and 4-37) both frames have yielded girders at the same level, 11^{th} floor, this helps the structure to have a more uniform drift response. This fact confirms that the strength reduction factor encouraged yielding in the girders in higher levels of the building. When yielding occurs in the top levels of a structure, the drift can be redistributed over a larger portion of the structure and improve the response.

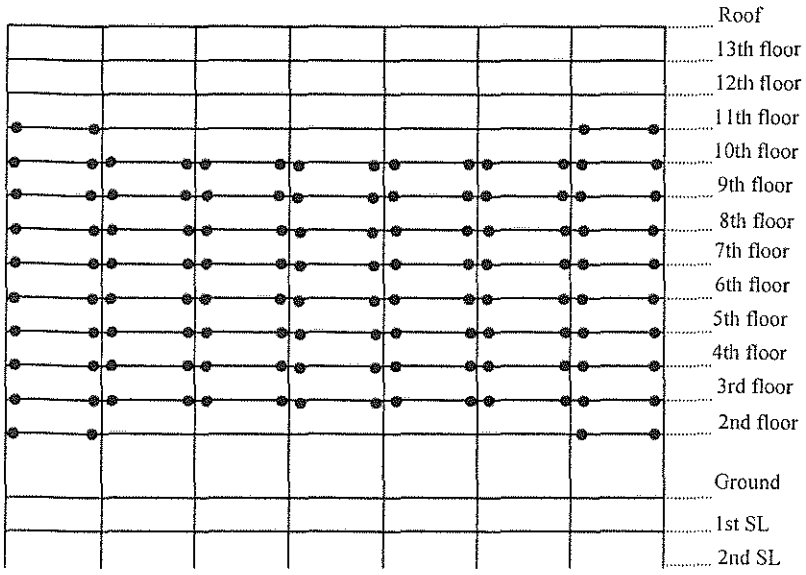

Figure 4-38. Yielding Profile for Modified Model C - Exterior Frame

In Figure 4-38 and Figure 4-39 it is observed that modified Model C has less yielded girders at the 11th floor than modified Model B. There are less yielded elements at the 11th floor for Model C, because the softer foundation helps to redistribute the deformations and demands on the structure.

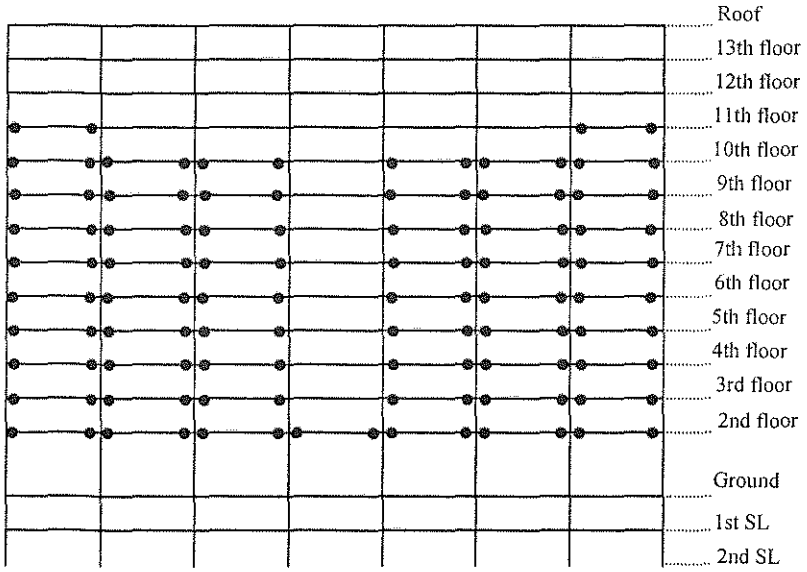

Figure 4-39. Yielding Profile for Modified Model C - Interior Frame

The primary difference between the unmodified Model C (Figure 4-8 and Figure 4-10) and the modified Model C (Figure 4-38 and Figure 4-39) is found in the highest level with yielded girders. The unmodified model has yielded girders up to the 9th floor for the exterior frame and up to the 8th floor for the interior frame. The modified model has yielded elements up to the 11th floor in both frames. As stated before the model with yielding at higher levels may have a better response because this encourages the structural mechanism to developed in the structure.

4.3.2.7. Deformed Shape and SDR for Original Northridge Building Record

Figure 4-40 shows the deformed shapes for the unmodified and modified models B and C. It appears that for this moderate earthquake demand the strength reduction factor does help to significantly reduce the drift at mid height while increase the drift at the upper floors.

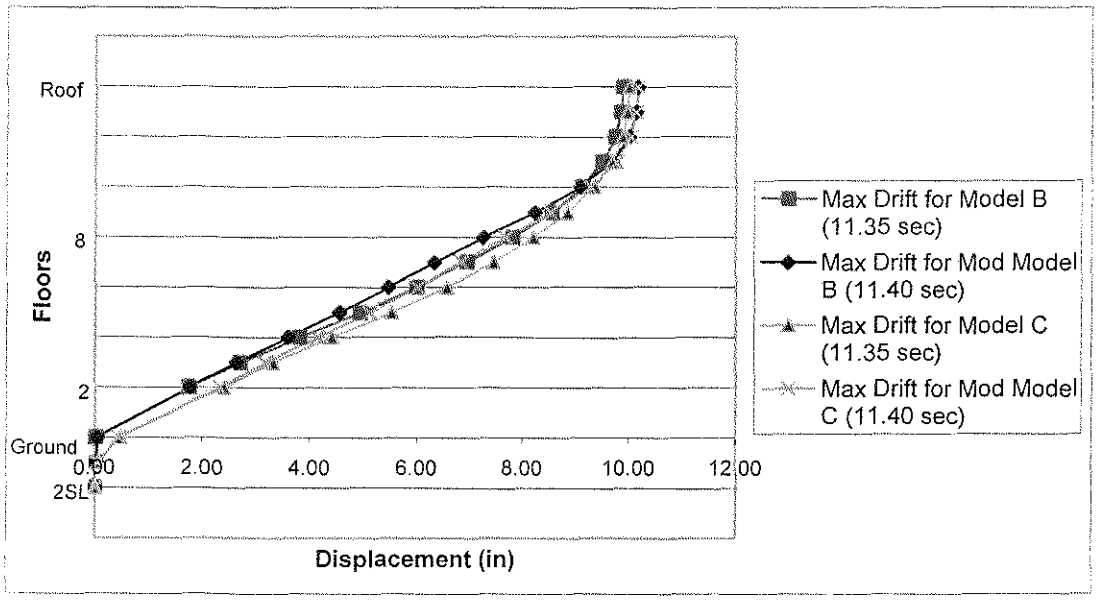

Figure 4-40. Deformed Shape for all Models Subjected to Building Acceleration Record (Northridge)

Figure 4-41 and Figure 4-42 show how the interstory displacements were reduced at mid- height and increased for the upper floors of the structure. The sublevels SDR remain almost constant for Model B and Model C. Yet the SDR for the first sublevel for Model B (stiffer foundation) was increased, this demonstrates how the redistribution of the drift is evident in all levels. For Model C, the SDR for both sublevels were reduced to could create a more uniform SDR for the floors above.

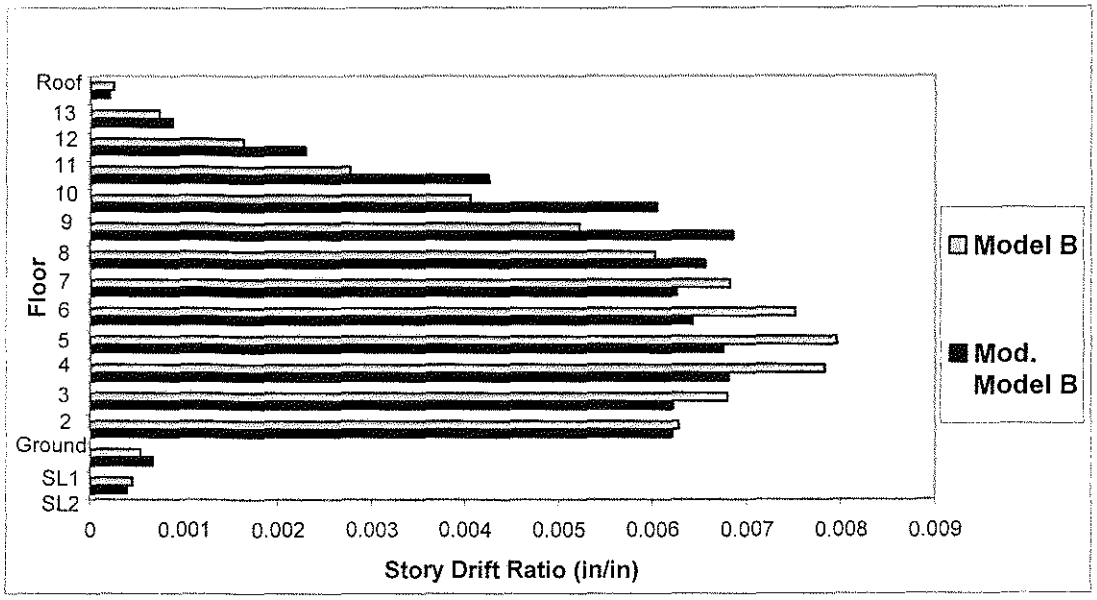

Figure 4-41. Comparison of SDR Values for Unmodified and Modified Model B

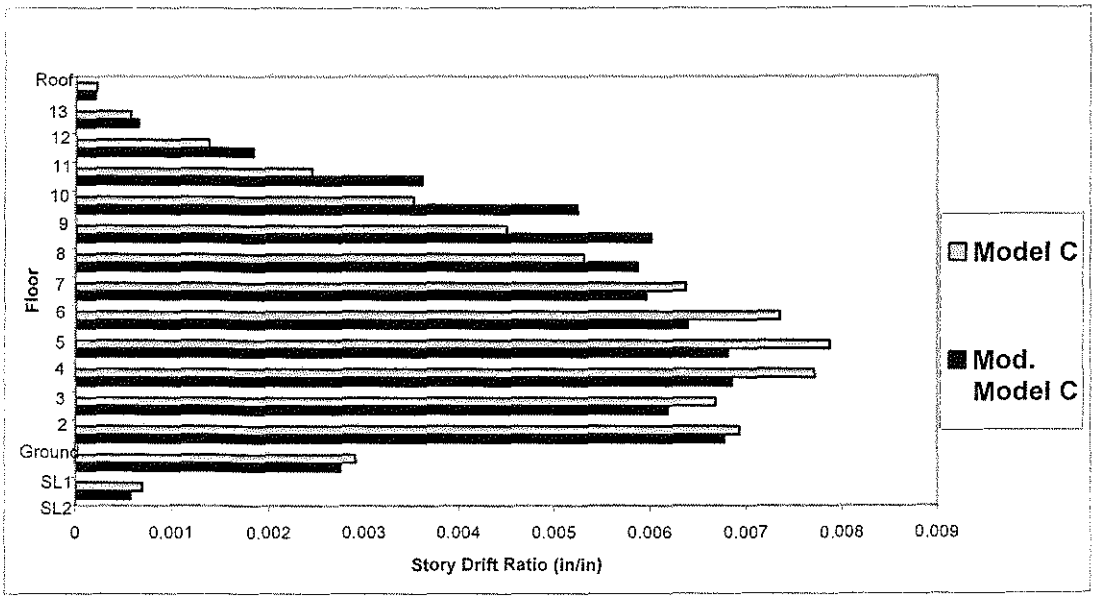

Figure 4-42. Comparison of SDR Values for Unmodified and Modified Model C

4.4. Summary

Chapter 4 shows how to implement the strength reduction factor in a 13 story structure and the restrictions that were used to apply the method. The results for different models and earthquake demands were analyzed and discussed. In general, it was shown that the strength reduction factor helps to improve the SDR for a structure subjected to several earthquake demands. The structures with stiff foundations are more sensitive to the strength reduction factor and showed a larger improvement.

5. CONCLUSIONS

The analysis of the results of Chapter 3 and Chapter 4 led to several conclusions about the modeling and model modification of a 13 story structure:

- The accurate modeling of the foundation is a key element in the structure with sublevels. It is not possible to ignore the influence of the structure-soil and or sublevel stiffness interaction and obtain a representative response for the target structure analyzed.
- The static and dynamic analyses for Models B and C had nearly identical yielding profiles and deformed shapes, this confirms the reliability of the static analysis.
- The strength reduction factor showed to have a strong influence in the response of a structure with a stiff foundation (Model B). This was shown in yielding profiles, deformed shapes and SDR.
- The structure with a soft foundation did not show improvement in its response after the strength reduction factor was applied to the model (Model C).
- The earthquake demand (intensity and frequency content) seems to influence the effectiveness of the strength reduction factor in improving the response of a structure.
- In general the strength reduction factor decreases the SDR values for mid-height floors and increases SDR for the upper floors.

The analysis of the obtained results of this study show the benefit of including a strength reduction factor in the design of structures. Yet, the improvement in the

structural response has a limit as showed the analysis of Pacoima Dam record. The target structure was not able to show a substantial improvement in its response because the reduction factor used was restricted by the gravity loads.

6. REFERENCES

Finn,W.D. Lian, G. Wu and T. Thavaraj. (1997). "Soil-Pile-Structure Interactions," Geothecnical special publication No.70, ASCE, pp. 1-22.

Han, Yingcai and Cathro, Derek.. (1997). " Seismic Behavior of Tall Buildings Supported on Pile Foundations", Geothecnical special publication No.70, ASCE, pp. 36-51.

Clough, R.W and Jhonston, S.B. (1966). "Effects of Stiffness Degradation on Earthquake Ductility Requirements", Proc., Japan Earthquake Engineering Symposium, Tokio, October 1966, pp. 195-198.

Otani, S. and Sozen, M.A. (1972). "Behavior of Multistory Reinforced Concrete Frames During Earthquakes." Tech. Report Struct. Res. Series No. 392, University of Illinois, Urbana, Ill.

Takeda, T., Sozen, M.A. and Nielsen, N.N. (1970). "Reinforced concrete response to simulated earthquakes." J. Struct. Div., ASCE, 96 (12), pp.2557-2573

Naeim, Farzad. (2000). "Response of Instrumented Buildings to Northridge Earthquake - An interactive Information System". California Strong Motion Instrumentation Program, DMG CD 2000-009.

Lopez, R. R.(1988). "Numerical Model for Nonlinear Response of R/C Frame-Wall Structures." PhD Thesis Submitted to the Graduate College of the University of Illinois, Urbana, Ill.

American Society of Civil Engineers. (2000) "Minimum Design Loads for Buildings and Other Structures." ASCE Standard.

USGS. http://groundmotion.cr.usgs.gov/SJO/movies/sjamovie.html

American Concrete Institute. (1999) "Building Code Requierements for Structural Concrete (318-99) and Comment (318R-99)" pp. 318/318R-81, 318/318R-82, 318/318R-92.

BSSC. (1997) "NEHRP guidelines for the seismic rehabilitation of buildings," Rep. FEMA 273 (Guidelines), Chapter 6, Washington, D.C.

Federal Emergency Managament Agency (2000). "Prestandard and Commentary for the Seismic Rehabilitation of Building", Washington, D.C.

American Society of Civil Engineers (2000). "Minimum Design Loads for Buildings and Other Structures", Reston, VA.

Ventura, Carlos E., Finn, W.D, Schuster, Norman D. (1995) "Seismic Response of instrumented structures during the 1994 Northridge, California, earthquake". Canadian Journal of Civil Engineering, Vol 22,1995, pp. 316-337.

Marsh, Jenelle N. (2001). "Correlating nonlinear static and dynamic analyses of reinforced concrete frames". Master of Science Thesis, University of Kansas.

Kuntz , Gregory L. (2001). "Analysis of method for improving the performance of reinforced concrete frame buildings during earthquakes". Master of Science Thesis, University of Kansas.

Saiidi, Mehdi, Sozen, Mete A. (1979) "Simple And Complex Models For Nonlinear Seismic Response Of Reinforced Concrete Structures." Doctoral Degree Thesis, University of Illinois.

Chowdhury, Asadul H. (1984) "Effect Of Foundation Flexibility On Dynamic Response Of Tall Buildings." International Symposium on Dynamic Soil-Structure Interaction, Minneapolis, pp 159-168.

Wolf, John P., Chongmin, Song. (1996) "Finite-Element modeling of Unbounded Media." John Wiley & Sons, Chichester, England.